Are we using the right fuel to drive hydrological models? A climate impact study in the Upper Blue Nile

Stefan Liersch[1], Julia Tecklenburg[1], Henning Rust[2], Andreas Dobler[2], Madlen Fischer[2], Tim Kruschke[3], Hagen Koch[1], and Fred Fokko Hattermann[1]

[1]Potsdam Institute for Climate Impact Research (PIK), Telegraphenberg A31, 14473 Potsdam, Germany
[2]Free University of Berlin (FUB), Institute of Meteorology, Carl-Heinrich-Becker-Weg 6-10, 12165 Berlin, Germany
[3]GEOMAR Helmholtz Centre for Ocean Research Kiel, Germany

Correspondence to: Stefan Liersch (liersch@pik-potsdam.de)

Abstract. Climate simulations are the fuel to drive hydrological models that are used to assess the impacts of climate change and variability on hydrological parameters, such as river discharges, soil moisture, and evapotranspiration. Unlike with cars, where we know which fuel the engine requires, we never know in advance what unexpected side-effects might be caused by the fuel we feed our models with. Sometimes we increase the fuel's octane number (bias-correction) to achieve better performance and find out that the model behaves differently but not always as was expected or desired. This study investigates the impacts of projected climate change on the hydrology of the Upper Blue Nile catchment using two model ensembles consisting of five global CMIP5 Earth System Models and ten Regional Climate Models (CORDEX Africa). WATCH forcing data were used to calibrate an eco-hydrological model and to bias-correct both model ensembles using slightly differing approaches. On the one hand it was found that the bias-correction methods considerably improved the performance of average rainfall characteristics in the reference period (1970–1999) in most of the cases. This also holds true for non-extreme discharge conditions between Q_{20} and Q_{80}. On the other hand, bias-corrected simulations tend to overemphasise magnitudes of projected change signals and extremes. A general weakness of both uncorrected and bias-corrected simulations is the rather poor representation of high and low flows and their extremes, which were often deteriorated by bias-correction. This inaccuracy is a crucial deficiency for regional impact studies dealing with water management issues and it is therefore important to analyse model performance and characteristics, the effect of bias-correction, and eventually to exclude some climate models from the ensemble. However, the multi-model means of all ensembles project increasing average annual discharges in the Upper Blue Nile catchment and a shift in seasonal patterns, with decreasing discharges in June and July and increasing discharges from August to November.

1 Introduction

Ethiopia is a country where about 80% of the population is engaged in the agricultural sector (Dile et al., 2013; Deressa et al., 2011), the main source of income for rural communities (Bryan et al., 2009). Around 90% of the country's grain is produced by smallholder farms. Subsistence and rain-fed farming systems dominate and, with few exceptions, irrigation is not practiced[1]. Consequently, agricultural and livestock production, people's livelihoods, and food security depend strongly on

[1]http://www.fao.org/wairdocs/ilri/x5548e/x5548e0k.htm

weather conditions, mainly on rainfall patterns such as amounts and timing. Hence, a large share of Ethiopia's population is very vulnerable to weather conditions and in particular to its inter-annual variability (Busby et al., 2014; Megersa et al., 2014; Headey et al., 2014; Zaitchik et al., 2012; Simane et al., 2012).

The Ethiopian highlands, where the Blue Nile is rising in, are considered as the water tower in East Africa. The Blue Nile, for instance, contributes about 55–65% of the flow of the Nile at the confluence with the White Nile (King, 2013; Sutcliffe and Parks, 1999). The river is therefore the most important water resource not only for Ethopia but also for the downstream riparian countries Sudan and Egypt. Water politics in the Nile basin have a long history and are a central geopolitical feature in this region (Gebreluel, 2014; Ibrahim, 2012). With growing populations, industrialisation, climate change and its variability, the situation becomes more and more tense (Gebreluel, 2014). Knowledge about availability of future water resources in this region and therefore studies providing insights into climate change and variability, and their impacts on the hydrology, are of outmost importance.

A review of future hydrological and climate studies in the River Nile basin is provided by Di Baldassarre et al. (2011) and a review on hydrological extremes in the Upper Blue Nile catchment (UBN) by Taye et al. (2015). Recent studies on climate change and variability in the UBN or its tributaries served different purposes. The studies by Mengistu et al. (2014); Taye and Willems (2012); Conway and Schipper (2011); Conway and Hulme (1993) investigated for instance trends of past climate change using observed and/or generated climate data. Diro et al. (2009) analysed the quality of rainfall data using two numerical weather prediction models. Another category of studies investigates the performance and projected trends of climate models (e.g., Conway and Schipper, 2011; Diro et al., 2011).

Studies performed to assess impacts of climate change in the UBN can be categorised into i) studies applying simple approaches, assuming for instance a fixed percentage of decrease or increase of a climatic variable or discharge (Jeuland and Whittington, 2014); ii) studies using a single climate model (e.g., McCartney and Menker Girma, 2012; Soliman et al., 2009; Abdo et al., 2009); and iii) studies analysing complex climate model ensembles (e.g., Teklesadik et al., 2017; Liersch et al., 2017; Aich et al., 2014; Mengistu and Sorteberg, 2012; Setegn et al., 2011; Beyene et al., 2010; Elshamy et al., 2009; Kim et al., 2008).

As a matter of fact, climatic variables such as air temperature, precipitation, and radiation simulated by global and regional climate models usually have a bias in the historical (reference) period (e.g., Addor and Seibert, 2014; Berg et al., 2012; Gudmundsson et al., 2012; Hagemann et al., 2011). Moreover, they often fail to adequately represent spatio-temporal dynamics at the regional scale. In climate studies, the absolute or relative changes between historical and projection periods are analysed and reported in the manner of: Model X projects a temperature increase of 2.5 Kelvin in 2021–2050 and an increase of 8% of rainfall relative to its reference period. Here, it does not matter whether model X was too cold/warm or too dry/wet during the reference period. Only the rate of change matters, which might be reasonable in this context. Moreover, in climate change studies it is nowadays common practice to analyse the entire available model ensemble and to calculate the multi-model mean which is superior to any one individual climate model (Pierce et al., 2009). Unfortunately, a daily multi-model mean climate time series does not serve as reasonable input to impact models operating at the daily time step. Therefore, the application of

climate model ensembles is always recommended for hydrological studies (Teutschbein and Seibert, 2010) and is nowadays considered as state of the art.

Quantitative and application-oriented impact studies require a certain accuracy of input data as well as adequate representation of the relevant processes by the models used. Already small biases in temperature or precipitation may lead to considerable biases in impact models (Maraun et al., 2010). Therefore, various bias-correction approaches were developed, particularly for hydrological applications (Piani et al., 2010; Dosio and Paruolo, 2011). The expectation of using bias-corrected input data is that they are quantitatively more precise than their uncorrected counterparts.

The authors of studies using complex model ensembles in the UBN, cited above, applied different approaches to generate climate input time series for hydrological modelling. Elshamy et al. (2009) used a distribution mapping approach to simultaneously downscale and bias-correct 17 CMIP3[2] GCMs (SRES A1B) and applied the corrected climate data to run the Nile Forecasting System in the UBN. The delta-change method was used by Mengistu and Sorteberg (2012) and Kim et al. (2008) to generate time series of temperature and precipitation used as input for hydrological modelling. Mengistu and Sorteberg (2012) used 19 GCMs of the CMIP3 model ensemble (SRES scenarios A2, A1B, and B1) to generate climate inputs for the SWAT model and Kim et al. (2008) used six GCMs (SRES A2) to run a monthly water balance model. Setegn et al. (2011) applied a downscaling approach for daily temperature and precipitation data to 15 CMIP3 GCMs (SRES scenarios A2, A1B, and B1) using a cumulative frequency distribution approach. They used the climate data to run the SWAT model in the Lake Tana basin. Beyene et al. (2010) performed a quantile mapping approach to bias-correct 11 CMIP3 GCMs (SRES A2 and B1) to run the VIC hydrological model for the entire Nile basin. Recently, Teklesadik et al. (2017) published a study comparing climate change impacts, particularly on actual evapotranspiration, using six hydrological models driven by the same four CMIP5 GCMs used in the study at hand. Liersch et al. (2017) used a climate model ensemble to analyse the impacts of the Grand Ethiopian Renaissance Dam on downstream discharges under current and future climate conditions based on the ten "best" global and regional climate models identified in this study.

The study at hand falls into the same category using most recent global and regional climate projections released for the IPCC 5th Assessment Report (IPCC, 2013). Uncorrected and bias-corrected climate simulations of five CMIP5[3] Earth System Models (ESMs) and ten uncorrected and bias-corrected Regional Climate Models (RCMs) from (CORDEX Africa[4]) were used to run the Soil and Water Integrated Model (SWIM), developed by Krysanova et al. (2005). The climate scenarios used by both model ensembles are the Representative Concentration Pathways (RCPs) RCP 4.5 and RCP 8.5 (van Vuuren et al., 2011; Meinshausen et al., 2011). Hence, we analyse 60 discharge simulations (2 RCPs, 15 uncorrected and 15 bias-corrected climate model runs) for the reference period 1970–1999 and two future periods 2030–2059 and 2070–2099.

The first objective of this study is to assess climate change and its impacts on the availability of future water resources in the UBN defined at gauge El Diem (Sudan Border). The second objective is to discuss the implications of using different model ensembles to project future discharges by comparing the results of the whole range of uncorrected and bias-corrected ESMs and

[2]http://cmip-pcmdi.llnl.gov/cmip3_overview.html?submenuheader=1

[3]http://cmip-pcmdi.llnl.gov/cmip5/

[4]http://start.org/cordex-africa/about/

RCM ensembles. Eventually an ensemble is assembled including only those members fulfilling certain performance criteria. These criteria are used to characterise the suitability of simulations for different purposes, such as for qualitative or quantitative studies. A qualitative impact study may have lower demands on the quality of climate simulations than a study investigating hydrological extremes or water management strategies. In the latter case, the requirements in terms of quantitative accuracy are much higher. The following questions were central to our investigations: a) What are the likely impacts of climate change on future discharges in the UBN? b) Is there an agreement on the signal of climate change impacts in the 21st century using different climate model ensembles? c) To what extent can bias-correction alter the magnitudes of change signals in hydrological simulations in the study area? d) In how far can we trust simulations that require a strong correction?

2 Study area

The entire Blue Nile River basin covers an area of about 296,000 km^2. The study area considered here is the Upper Blue Nile catchment (UBN) defined by gauge El Diem at the border between Ethiopia and Sudan that covers an area of 172,000 km^2. Elshamy et al. (2009) estimates a catchment area of 185,000 km^2 and Mengistu and Sorteberg (2012) an area of 174,000 km^2 for the UBN. These discrepancies are certainly based on different digital elevation models and GIS algorithms used to delineate the catchment area and thus may add to the uncertainties of such studies, which are not easily quantifiable. In Fig. 1, the UBN is encircled by a red line. In addition, it shows the 576 subbasins that were delineated for the hydrological modelling exercise, the three gauging stations used to calibrate the hydrological model, and the coordinates of the climate data grid. The source of the Blue Nile River is Lake Tana in the Ethiopian highlands and the catchment is located in the north-western part of Ethiopia (Taye and Willems, 2012). It drains a major part of the western highlands (Sutcliffe and Parks, 1999) that is predominantly governed by a unimodal rainfall regime depending on the movement of the Intertropical Convergence Zone (ITCZ). The interannual variability of annual rainfall amounts in the Ethiopian highlands is high (Zaitchik et al., 2012) and ranges between 800 and 2200 mm and the elevation of the UBN varies from 4000 to 500 m.a.s.l. (Taye and Willems, 2012). The river has a length of almost 1000 km from Lake Tana outlet to the Sudan border.

3 Methods

3.1 Data

Freely available WATCH Forcing Data (WFD) (Weedon et al., 2011) based on ERA-40 (Uppala et al., 2005) reanalysis and climate observations were used to bias-correct five ESMs and ten RCM runs and to calibrate and validate the hydrological model SWIM (Soil and Water Integrated Model), developed by Krysanova et al. (2005). Although the quality of WFD varies in space (Rust et al., 2015), this gridded product with a spatial resolution of 0.5° was used as input because observed climate data were not available for this study. The SRTM digital elevation model (Jarvis et al., 2008) was used to delineate the 576 subbasins and to derive some terrain-specific parameters. Required soil parameters were derived from the Digital Soil Map of the World (FAO et al., 2009) and land use cover data were reclassified from Global Land Cover (GLC2000) (Bartholomé and

Belward, 2005). Observed monthly discharge data for model calibration and validation were provided by the Global Runoff Data Centre (GRDC[5]).

3.2 Hydrological model

The Soil and Water Integrated Model (SWIM), developed by Krysanova et al. (2005), is a semi-distributed, process-based eco-hydrological model that operates at the daily time step. It was developed on the basis of the MATSALU (Krysanova et al., 1989) and SWAT (Arnold et al., 1993) models and is continuously further developed and adapted to new or specific requirements (Krysanova et al., 2015). Hydrological response units (HRU), considered as areas with similar hydrological characteristics, are the smallest model units where all hydrological, nutrient, and vegetation processes are calculated. There is no lateral interaction between HRUs but area-weighted daily fluxes are calculated and aggregated at the subbasin scale and routed through the river network. SWIM distinguishes three flow components: surface runoff, subsurface runoff, and contributions of the shallow groundwater aquifer. Actual evapotranspiration is determined by simulated soil evaporation and transpiration from the vegetation cover. Water percolating from the shallow groundwater aquifer into the deep groundwater aquifer is lost from the system but is considered in the water balance.

A reservoir module, developed by Koch et al. (2013), was incorporated in SWIM and parameterised to better account for Lake Tana's storage effects and to consider the impact of the weir at the Lake's outlet in future simulations that was constructed in the year 1996.

Radiation data required by SWIM as essential climate input were not available in all RCM runs. To maintain consistency and comparability in hydrological simulations, daily radiation data were computed after Hargreaves and Samani (1985) from daily minimum and maximum air temperature and the latitude of the respective subbasin. The simulated radiation data were calibrated to fit average annual observed radiation data of about 1800 kWh m^{-2}.

3.3 Climate models

The ESM ensemble used in this study consists of following five CMIP5 models: GFDL-ESM2M, HadGEM2-ES, IPSL-CM5A-LR, MIROC-ESM-CHEM, and NorESM1-M. Projections of these five ESMs were linearly downscaled and bias-corrected by Hempel et al. (2013) in the frame of the Inter-Sectoral Impact Model Intercomparison Project (ISIMIP)[6] (Warszawski et al., 2014). The uncorrected ESM simulations were interpolated to the WFD 0.5° grid.

Table S1 in the Supplement provides an overview of the RCM runs organised by the CORDEX Africa initiative[7]. The ensemble consists of four RCMs driven by different ESMs. The RCM SMHI-RCA4 was driven by seven ESMs, CanRCM4 by CanESM2 and the RCMs KNMI-RACMO22T and DMI-HIRHAM4 by EC-EARTH. The ten RCM runs were bias-corrected by the authors of this manuscript. Table S2 shows the model IDs of all 15 climate models used in some figures and tables.

[5] http://www.bafg.de/GRDC/EN/Home/homepage_node.html

[6] https://www.pik-potsdam.de/research/climate-impacts-and-vulnerabilities/research/rd2-cross-cutting-activities/isi-mip

[7] http://start.org/cordex-africa/about/

3.4 Climate scenarios

For both the global and regional climate model ensembles, the two scenarios RCP 4.5 and RCP 8.5 were used because they represent a broad range of uncertainties with regard to possible future pathways and related climate projections. According to van Vuuren et al. (2011) and Meinshausen et al. (2011), RCP 4.5 represents the medium stabilisation scenario (stabilisation without overshoot pathway leading to +4.5 W m^{-2} radiative forcing (relative to pre-industrial forcing) and ~650 ppm CO_2 eq by 2100) and RCP 8.5 the highest emission scenario (rising radiative forcing pathway leading to +8.5 W m^{-2} and ~1370 ppm CO_2 eq by 2100) assuming no stabilisation in global GHG emissions.

3.5 Bias-correction

Despite regional downscaling to finer resolution, RCM simulations often show considerable biases when compared to observed data (Addor and Seibert, 2014; Christensen et al., 2008). A review on bias-correction methods (linear scaling, local intensity scaling, power transformation and distribution or quantile mapping) provide Teutschbein and Seibert (2012). The authors conclude that the distribution or quantile mapping method achieves the best performance for most of the selected criteria. Although quantile mapping is a successful method to improve the representation of daily rainfall characteristics, it fails to correct multi-day and inter-annual variables, such as mean maximum 4-day precipitation, mean minimum 14-day precipitation, and inter-annual variability (Addor and Seibert, 2014). The drawback that all approaches have in common is that they are based on the stationarity assumption which presumes that future physical processes in the atmosphere are comparable to the period used to correct the simulations. Bias-correction of climate simulation data is nowadays a widely used practice in hydrological impact modelling but it should be treated with caution. As Maraun et al. (2010) point out, the origins of the bias in climate simulations (mathematical formulations in climate models) are not solved by the post-processing and may disrupt internal physical coherence between weather variables. Hence, the corrections are usually based on wrong reasons (Addor and Seibert, 2014). Alternatives to bias-correction are so-called delta-change methods. Sophisticated approaches of this method are described by Anandhi et al. (2011), Bosshard et al. (2011), and Chiew et al. (2009).

3.5.1 Bias-correction of ESMs

Bias-corrected data of five CMIP5 ESMs were available and provided by ISIMIP. In a first step ESM data were linearly interpolated to the WFD 0.5° grid implementing the standard Gregorian calendar. Temperature data were corrected using a trend-preserving additive approach where monthly mean values were adjusted for a systematic bias by adding a grid-point and month-specific constant offset. Thereby, the absolute projected temperature changes of the ESMs are not changed. The daily variability of ESM temperatures was adjusted to reproduce WFD variability by adding a monthly correction factor on temperature anomalies.

Precipitation data were corrected using a multiplicative approach where monthly mean precipitation was multiplied with a grid-point and month-specific constant correction factor. Relative changes projected by the ESMs are thereby preserved. A known problem of this method is that extraordinary high values of daily precipitation can occur in the bias-corrected simulation

if very high simulated daily precipitation data are multiplied with high correction factors. Therefore, the correction factor was limited to a value of 10. Remaining extremely high daily precipitation values were truncated to 400 mm. After the method introduced by Piani et al. (2010), daily precipitation variability and the frequency of dry days was corrected by applying a transfer function to fit the normalised simulated time series of wet months to the normalised WFD time series. A more detailed description of the bias-correction procedure applied to the five CMIP5 ESMs used in this study provides Hempel et al. (2013).

3.5.2 Bias-correction of RCMs

Precipitation biases in most CORDEX RCMs show a high seasonality for grid boxes within the evaluation domain of the UBN. This limits a bias correction based on seasonal or annual means. However, as some of these grid boxes do show almost no precipitation events for single months, a harmonic-based bias correction method analogously to the one applied to temperature is not feasible for precipitation. Furthermore, this results in a large uncertainty in the estimation of the corresponding monthly biases. Thus, based on the recommendation from Dobler and Ahrens (2008), a bias correction is only applied on months and grid boxes with more than 100 rainy days (rainfall above 1 mm/day) within the calibration period (1951–2001).

The method applied is based on a local rainy day intensity scaling, correcting the frequency of rainy days and the mean precipitation on rainy days to fit the observed values in a specific calibration period (Schmidli et al., 2006). Details on the implementation and an evaluation are given in Dobler and Ahrens (2008). The method has been successfully applied before as a downscaling and bias correcting method for precipitation in alpine regions (Dobler and Ahrens, 2008; Dobler et al., 2011).

The underlying idea is the assumption of a smooth seasonal cycle for the variables simulated by the RCM and the observational reference (WFD). These cycles are modelled with a series of harmonic functions using vector generalised linear models (Yee, 2015) and the difference in cycles between an RCM reference simulation and the observational product is used for bias correction of the RCM projection.

The seasonality in the location parameter of a quantity (i.e. the expectation value in case of a Gaussian distribution) can be modelled as

$$\mu(t) = \mu_0 + \sum_{k=1}^{K} \mu_k \sin(k\,\omega\,t) + \sum_{l=1}^{L} \mu_l \cos(l\,\omega\,t) \tag{1}$$

with $\omega = \frac{2\pi}{365.25}$, $t = 1, \ldots, 366$ being the time variable running over all possible days of the year; K and L are the orders of the harmonic function expansion for μ. A scale parameter σ can be modelled analogously in this framework. The result is a climatological distribution, i.e. a description of the probability distribution throughout the year.

Selection of orders K and L are based on a 10-fold cross validation using Continuous Rank Probability Score (CRPS, Wilks, 2011) as cost function. The difference in parameters between the RCM reference and the observational product (WFD) is subtracted from the parameters of the RCM projections for bias correction. A quantile mapping (e.g., Vrac and Friederichs, 2015) now maps the values from the uncorrected to the corrected climatological distribution.

Particular care needs to be taken when correcting minimum and maximum temperature to avoid inconsistencies such as $T_{max} < T_{min}$. Here, a variable transformation ensures physical consistency:

$$T_1 = \log(T_{max} - T) \tag{2}$$

$$T_2 = \log(T - T_{min}) \tag{3}$$

After bias correcting T_1 and T_2, corrected values for T_{max} and T_{min} can be obtained by back-transforming the variables.

3.6 Evaluating the suitability of climate simulations

Evaluating the suitability of climate simulations for regional impact studies is a process including seemingly objective components (e.g., analysing performance criteria) and subjective components (choosing criteria and setting their thresholds). Data visualisation and interpretation by the user might be considered as a mixture of both objectivity and subjectivity. The choice of periods used as reference and future projection does also influence the results. The former is often predetermined by data availability or conventions and the latter usually by the client. Moreover, there are uncertainties with regard to quality of the dataset used as comparison baseline, mostly observed and/or generated climate data.

Evaluation of climate model performance is complicated by the fact that climate simulations cannot be compared to the reference dataset on a real-time daily, monthly, or annual basis, as it is common practice with discharge simulations in hydrological modelling. Climate simulations are not supposed to reproduce or predict the weather at a certain day, month, or year. Hence, only statistical parameters, summarised over a period of usually 30 years (e.g. the annual cycle represented by average daily or monthly time series) or the mean, quantile values, and standard deviation of the entire daily time series can be used as a basis for comparison.

In the first step of climate model evaluation, daily and monthly precipitation characteristics of uncorrected (UC) and bias-corrected (BC) climate simulations were compared to monthly WFD characteristics (reference climate). In a second step, SWIM was employed to simulate daily discharge using all climate simulations for reference and future periods. Since the main purpose of this study is to assess climate change impacts on the hydrology, using hydrological performance indicators to evaluate climate simulations is a straightforward way. A similar approach was used by Elshamy et al. (2013) who used a GLUE-like methodology to exclude and weigh climate model performance. Another benefit of this approach is that a spatially semi-distributed hydrological model does not only account for temporal but also for spatial patterns of climate inputs. Therefore, the annual cycle represented by daily ($n = 365$) discharge simulations (sim) averaged over the 30-years reference period, was compared against the baseline simulation using WFD (ref). The performance criteria applied to these time series are: Coefficient of determination (R^2), $PBIAS$, standard deviation (SD), and the normalised SD of discrepancies (SD_D) or the centred root mean square errors, respectively.

The characteristics of daily discharges were analysed using flow duration curves (FDCs), where every single discharge value is related to the percentage of time it is equalled or exceeded (Smakhtin, 2000). FDCs summarise discharge variability of a

time series and display the complete range from low flows to flood events. In order to analyse and visualise average, low, and high flow characteristics, 17 percentile values ($Q_{0.01} - Q_{99.99}$) were used to compute FDCs based on the entire daily discharge time series of the 30-years reference period. This method was applied to assess whether model performance is suitable to study non-extreme discharge conditions (NED) and/or high and low flow situations as well as their extremes.

$$PBIAS = \frac{\sum_{i=1}^{n}(sim_i - ref_i) * 100}{\sum_{i=1}^{n}(ref_i)} \tag{4}$$

$$SD_D = \frac{SD(sim_i - ref_i)}{SD_{ref}} \tag{5}$$

In addition to the criteria used to evaluate model performance in the reference period, it is also important to consider model behaviour in future periods. In fact, unexpected behaviour in projection periods was observed in several simulations, particularly in some BC simulations. The hypothesis is that the stronger the necessity of bias-correction the higher the risk that the BC simulation will show unexpected behaviour in future periods. Therefore, another criterion was introduced that indicates the rate of change of $PBIAS$ between future and reference period. Note that the definition of threshold values is somewhat subjective and was influenced by the simulation results of the model ensemble. However, if the thresholds would have been set more critically, almost no climate model would have passed the evaluation process successfully. The model selection process and the definition of criteria thresholds are described in the following section.

3.7 Model selection

Beside analysing the impact of climate projections on future discharges using the whole UC and BC ESM and RCM ensembles, a climate model ensemble was assembled containing only those models that fulfil the criteria and their thresholds defined below. In order to become a member of the selected ensemble, a model must basically achieve all the following three criteria:

- Seasonality: The annual cycle based on average daily discharge simulations must achieve $R^2 \geq 0.85$. Models with $R^2 < 0.85$ are assumed to represent discharge seasonality only poorly.
- Volumetric deviation: Average daily discharge simulations must achieve a $PBIAS \leq \pm 30\%$.
- Non-extreme discharges (NED): NED represent discharge conditions between FDC percentile values between $> Q_{10}$ and $< Q_{90}$ ($Q_{20}, Q_{30}, ..., Q_{80}$). Percentiles in this range should not deviate more than $\pm 30\%$ from WFD discharge simulation.

Models meeting these three criteria are assumed to be suitable for a qualitative impact assessment and are indicated in column pre (pre-selection) in Table 1. In addition, the columns HF (high flows, FDC percentiles $Q_{10}, Q_5, Q_1, Q_{0.1}, Q_{0.01}$) and LF (low flows, FDC percentiles $Q_{90}, Q_{95}, Q_{99}, Q_{99.9}, Q_{99.99}$) indicate whether a particular model is further adequately

representing extreme discharge conditions and might be used for specific investigations. Again, the FDC values in the respective range should not exceed the threshold of $\pm 30\%$.

After simulating discharges using all climate scenarios it was found that several simulations project enormous increase in annual river discharge already in the period 2030–2059. This was particularly the case in simulations where bias-correction resulted in stupendous increase of extreme daily rainfall and therefore extraordinary high peak discharges. Hence, another criterion was defined representing the rate of change. Simulations where average annual discharges changed by more than $\pm 30\%$ in the period 2030–2059 (RCP 8.5) relative to the reference period were omitted from the selected ensemble, even if the first three criteria were achieved. This criterion is represented in Table 1 in column *Change*, which reveals that always both UC and BC models either achieve or not achieve this criterion.

4 Results

4.1 Model calibration and validation

The eco-hydrological model SWIM was calibrated to three discharge gauges in the UBN: 1. downstream Lake Tana, 2. Kessie, and 3. El Diem. Due to limited data availability, the model was calibrated to the monthly time step using a semi-automated approach. The calibration (1981–1986) and validation (1987–1992) periods for gauge El Diem were on the one hand chosen according to data availability and on the other hand to cover periods of wet and dry years. Data availability for the gauges Lake Tana and Kessie were limited to the years 1969–1975 and 1976–1979, respectively. The gauges were successively calibrated where a parameter sensitivity analysis was performed in a first step to assess reasonable parameter ranges as boundary conditions for the automatic calibration algorithm PEST (Model-independent parameter estimation & uncertainty analysis software)[8]. The objective functions to measure model performance are the Nash-Sutcliffe efficiency (NSE) (Nash and Sutcliffe, 1970) and PBIAS, where NSE was the primary criterion.

Figure 2 shows the results of monthly and average monthly discharges at gauge El Diem for calibration (left panel) and validation (right panel). According to Moriasi et al. (2007), NSE values of 0.92 (calibration) and 0.90 (validation) are considered as *very good* for the monthly time step. The same classification is achieved for the volumetric errors in both periods. The percent bias (PBIAS) between simulated and observed data is -6.7% (calibration) and -14.4% (validation). SWIM simulates peak discharges adequately in most years with few exceptions of rather large underestimation in the years 1983, 1987, and 1988. One explanation for this is the lack of accuracy of WFD inputs and/or observed discharge in some years. The simulated amount of water percolating into the deep aquifer is about 7% in average. Without this recharge component, it was not possible to achieve good simulations during the dry period.

The Figures S1 a) and b) in the Supplement show the calibration results for the gauges downstream Lake Tana and Kessie. The available GRDC discharge time series for both gauges are rather short and in the case of Tana, the data of the years 1973–1975 are not reliable. Compared to the discharge data given in Dile et al. (2013) and Setegn et al. (2011), maximum discharges

[8] http://www.pesthomepage.org/

are usually around 200–250 m^3s^{-1}, as is it the case in the years 1969–1972 (Fig. S1a). Monthly WFD precipitation volumes do not explain the high discharges observed in the last three years. Hence, only the first four years were used for calibration, where an NSE of 0.67 and a PBIAS of 23.1% were achieved. Monthly discharges at gauge Kessie in the four years where GRDC data were available are underestimated by -18.8% and achieved an NSE of 0.92. According to Moriasi et al. (2007) the results for the two gauges can be classified between *good* and *very good*.

4.2 Model performance

4.2.1 Performance of daily and monthly precipitation

Monthly medians and average annual precipitation sums of UC ESM and RCM simulations deviate sometimes strongly from WFD (see Figures S2, S3, and S4 in the Supplement). The underlying data for the boxplots are monthly precipitation sums of the 30-years reference period averaged over the UBN catchment area. Bias-correction improved the performance of both indicators considerably in both model ensembles. Deviations of average annual precipitation of all BC ESMs are lower than $\pm 2\%$. The results for the BC RCM ensemble are more diverse. Five RCMs deviate $\leq \pm 2\%$, three RCMs $\leq \pm 5\%$, and two RCMs $\leq \pm 7\%$

Despite the improvement of monthly medians and average annual precipitation sums, bias-correction increased the range of monthly precipitation sums critically in several models in both ensembles. This phenomenon can be observed particularly if the deviation of monthly medians between UC simulation and WFD is rather large (e.g. IPSL from May to October, MIROC in July, NorESM in July and August). The effect of increasing variability of monthly precipitation sums is even higher with the method used to bias-correct RCMs and is true for all RCMs (Figures S3 and S4). Noticeable are also the extreme outliers in many models generated by both correction methods.

Not all UC models do adequately represent the unimodal rainfall regime in the UBN. UC NorESM shows for instance a distinct bimodal regime which is also visible but less pronounced in GFDL and MIROC (Fig. S2) and only weakly visible in MIROC/RCA4 (Fig. S4). Although bias-correction eliminated this deficiency, it is questionable at what costs. The physical basis was certainly disrupted by the correction method applied.

The Tables S3 and S4 in the Supplement show following statistical parameters of daily precipitation averaged over the catchment: Average number of days with precipitation >1 mm per annum $nDays > 1mm$, average daily precipitation ave, maximum daily precipitation max, standard deviation SD, average precipitation in July, August, and September $ave(JAS)$, and the standard deviation of daily precipitation in July, August, and September $SD(JAS)$. Where Table S3 shows absolute values, Table S4 shows the differences to WFD precipitation (sim-WFD). The two SD parameters were computed by division SD_{sim}/SD_{WFD}. The Tables show for instance that maximum daily precipitation is underestimated by all UC models except by MIROC. Bias-correction resulted in overestimation in 13 out of 15 models. All BC RCMs overestimate maximum daily precipitation, many of them significantly. Yet the differences in average daily precipitation of BC simulations are, with exceptions, usually rather small. Large deviations in maximum daily precipitation and in the number of rainy days at the same time, while achieving only small differences in average daily precipitation, indicate that the distribution of daily rainfall can differ

sometimes strongly among simulations. It is also noticeable that the SD of daily precipitation of all UC models is lower than the WFD SD. Almost all BC simulations show higher SD than the UC simulations where all ESM SD are still lower than WFD SD and all RCM SD greater or equal than WFD SD.

4.2.2 Performance of average daily discharge using UC and BC climate input

Bias-correction improved the performance of averaged daily discharge simulations ($n = 365$) considerably for all members of the ESM ensemble and for most members of the RCM ensemble. Figures 3 and 4 show the simulated hydrographs in the reference period comparing UC and BC simulations with WFD using R^2 and $PBIAS$ to indicate discharge performance of the annual cycle.

All UC discharge simulations using ESM climate input, except the one based on GFDL, underestimate average annual discharges, which is indicated by negative $PBIAS$ values (Fig. 3). Largest deviations shows IPSL with a $PBIAS$ of -84%. All other models deviate less than 30% from WFD discharges. R^2 values indicate that seasonal discharge patterns are more or less adequately represented by all models, except by NorESM which simulates a bimodal regime with a small peak in June and a high peak in October instead of one single major peak between August and September. Peak discharges simulated with GFDL and MIROC climate input occur approximately four weeks later than the peak simulated with WFD. Discharges simulated with HadGEM achieve an R^2 of 0.98 but are too low during the high flow season. Another example is the UC IPSL model which achieves an R^2 of 0.9 although it underestimates discharge by -84%. Hence, high R^2 values can be misleading if not combined with a volumetric criterion, such as $PBIAS$.

On contrast to ESMs, the majority of discharge simulations based on UC RCMs overestimate average annual discharges in the reference period (Fig. 4). The deviations of six UC RCMs are larger than 30%. However, seasonal discharge patterns are generally better represented using UC RCM climate input than UC ESM input. The lowest UC RCM R^2 value is 0.93 compared to an R^2 of 0.49 by NorESM of the UC ESM ensemble. Hence, bias-correction improved R^2 values only slightly for 50% of RCMs. In 60% of the cases, the volumetric deviation ($PBIAS$) of BC RCMs is significantly lower than in the corresponding UC models. Based on these two indicators, the performance of BC RCM simulations is generally better than UC RCMs. However, there is a strong tendency of peak flow overestimation in six out of ten BC RCMs which is not captured by R^2 and $PBIAS$. Therefore, a visual assessment of hydrographs is important as well as an analysis of daily discharge characteristics using FDCs (see following section).

Taylor diagrams (Taylor, 2001) are another method to visualise model performance showing three performance indicators (R^2, normalised SD, and SD_D) in a single plot (see Fig. 5). They facilitate the visual assessment of model performance where outliers can be easily identified. A model having similar statistical characteristics as the reference dataset would be represented by a point at 1.0 on the x-scale and 0.0 on the y-scale. However, interpretation of normalised values is difficult in terms of numerical thresholds but Fig. 5 a) identifies UC IPSL and UC NorESM clearly as outliers. IPSL is, for instance, an outlier because it shows deficiencies at representing SD (0.25 where 1.0 would be ideal) and SD_D (0.79 where 0.0 would be ideal). UC NorESM performs poorly in terms of all indicators. After bias-correction all ESMs show rather good performance (see Fig. 5 b). Except BC IPSL, all models have lower SD than WFD. The characteristics of RCMs are different. Half of the UC

RCMs SD (Fig. 5 c) deviate more than ± 0.25 from standardised WFD but perform much better in terms of R^2. Interestingly, after bias-correction (Fig. 5 d), all models show a higher SD than WFD, which is consistent with higher SD of daily rainfall as described in the previous section.

4.2.3 Flow duration curves

FDCs are employed here to analyse and characterise strengths and weaknesses of daily discharge simulations with regard to NED conditions, high flows, low flows and their extremes. Fig. S5 in the Supplement shows FDCs of all ensembles where the black line represents simulations using WFD. At least one obvious outlier can be clearly identified in both UC ensembles (IPSL and CanESM2-RCA4). Apart from the outliers, NED characteristics are slightly better represented by the UC ESM ensemble (Fig. S5 a) than by the UC RCM ensemble (Fig. S5 c). Most of the UC RCMs tend to overestimate NED and low flows. At a first glance, the biases were significantly reduced by the correction methods (Fig. S5 b and d), especially for NED. However, compared to UC simulations, the correction led to higher biases in the high and low flow segments and especially in their extreme values. Note that a logarithmic y-scale is used where large deviations in the extreme high flow section appear rather small on this plot although they are in fact extremely high.

Figure 6 overcomes this problem by showing relative deviations of FDCs between discharge time series simulated with climate model inputs and the baseline using WFD. The values corresponding to Fig. 6 provide the Tables S5 to S8 in the Supplement. Assuming that deviations in the range of $\pm 30\%$ are tolerable, there is not a single UC model (Fig. 6 a and c) which fulfils these requirements for all percentile values. However, the UC ESMs MIROC and HadGEM (Fig. 6 a) show acceptable deviations ($\pm 30\%$) in NED conditions but there is not a single UC RCM representing NED conditions in the given range (Fig. 6 c). The best UC RCM result was achieved with NorESM1-RCA4. The Figures 6 b) and d) show that bias-correction was successful in correcting the biases of NED for all ESMs and seven out of ten RCMs. The correction method applied to ESMs leads to different patterns in the high and low flow sections compared to the method used to bias-correct RCMs.

Between Q_1 and Q_{10} (high flows), the BC ESMs tend to underestimation (but in the given range of acceptable deviations) whereas BC RCMs do overestimate flows corresponding to these percentiles. There is not a single BC RCM that represents Q_1 conditions in the given range of $\pm 30\%$. The smallest overestimation for Q_1 is 52.4%. All BC RCMs do strongly overestimate extreme high flows $Q_{0.1}$ and $Q_{0.01}$. The highest $Q_{0.01}$ overestimation is 656.9% and the lowest 100.4% (Table S8). The BC ESMs perform better in the extreme high flow segments. But only GFDL and HadGEM2 simulate $Q_{0.1}$ values in the acceptable range and only HadGEM2 for $Q_{0.01}$ (Table S6).

In the low flow section (between Q_{90} and Q_{99}) there is no BC ESM performing adequately for all percentile values. Except HadGEM2 that overestimates low flows, the other models tend to underestimation. Extreme low flows ($Q_{99.9}$ and $Q_{99.99}$) are only represented by GFDL within the acceptable range. The BC RCMs do all underestimate low flows, where four models are within the acceptable range of deviations for Q_{95} there is only one model within this range for Q_{99} (CanESM2-RCM4). Extreme low flow conditions ($Q_{99.9}$ and $Q_{99.99}$) are only represented adequately by EC-EARTH-RCA4, the other RCMs severely underestimate extreme low flows.

Summarising the evaluation of model performance based on FDCs it can be stated that bias-correction improved the performance of simulated NED significantly. However, with few exceptions, both bias-correction methods did not improve the performance of high and low flows. This is particularly true for extreme values which are strongly exaggerated in most cases.

4.3 Temperature, precipitation, and evapotranspiration projections

Figures 7, 8, and 9 show precipitation, temperature, and actual evapotranspiration projections of the selected model ensemble for the 21st century for RCP 4.5 and RCP 8.5 as anomalies to the reference period in the UBN. They indicate the total range of change and the 5-year moving average (MA5) for both scenarios. The precipitation MA5 does not show a distinct trend of change over the century but average annual precipitation is projected to be up to 100 mm (~7%) higher than in the reference period. The increase is only marginally higher in RCP 8.5 than in RCP 4.5. In Fig. S6 it is shown that maximal only three out of 15 UC climate models project decreasing average annual precipitation. The multi-model mean of the CMIP5 ESM ensemble projects increasing annual precipitation of 5% (6%) and 8.4% (15.6%) under RCP 4.5 and RCP 8.5 in 2030–2059 and (2070–2099), respectively. Fig. S7 shows where the five ESMs used in this study are situated within the entire CMIP5 ensemble. It is noticeable that only three out of 26 ESMs show declining precipitation trends under RCP 8.5.

Projected surface air temperatures show a clearly increasing trend over the 21st century in both RCPs. Compared to the reference period, the multi-model mean of the selected ensemble projects an increase of 1.7 K (1.5 to 1.9 K) in RCP 4.5 and 2.2 K (1.9 to 3.5 K) in RCP 8.5 in 2050. At the end of the century average temperatures climb up to 2.5 K (1.9 to 4.1 K) under RCP 4.5 and 4.9 K (3.0 to 6.5 K) under RCP 8.5. The multi-model mean of the CMIP5 ESM ensemble projects increasing average annual temperatures of 1.6 K (2.3 K) and 1.7 K (3.9 K) under RCP 4.5 and RCP 8.5 in 2030–2059 (2070–2099), respectively.

Although surface air temperature increases already until 2050 in both scenarios by up to 2.2 K, actual evapotranspiration remains rather stable on the level of the reference period. Only in the second half of the 21st century the projected values increase by up to 50 mm per annum. Hence, it can be concluded that actual evapotranspiration is already at its maximum and can only increase if water availability increases, too, as is the case after 2050.

4.4 Impact of bias-correction on discharge projections

Figures 10 and 11 show projected discharge changes of each single model under RCP 8.5 in the period 2030–2059. The changes are relative to the models' reference period. The figures allow to investigate the changes between reference and future period of UC and BC models as well as the differences of projected changes between UC and BC simulations. The indicators R^2 and $PBIAS$ are not used to measure the performance but indicate the magnitude of change between reference and projection period.

The IPSL model shows the largest deviations between future and reference period (Figure 10) for both UC and BC simulations. The UC IPSL model projects an increase of 95.4% in average annual discharge. A visual assessment supports the previously made assumptions that the IPSL model does not provide adequate climate simulations in the study area. This is true for both UC and BC climate simulations. Aich et al. (2014) applied the same five BC ESMs in four large African River basins and found that also in the Niger basin (comparable climate zone as the Blue Nile River) one of the five models projects

extreme and unexplainable changes although it performed adequately in the historical period. In the case of the Niger River basin, it was the MIROC model that behaved awkward in the projection period whereas the IPSL behaved in the range of the other models.

The HadGEM2 model is the only model where bias-correction changed the sign of the discharge signal. The simulation with UC climate input projects a decrease of average annual discharges of -2.9% and the BC simulation an increase of +2.2%. Interesting are the results of the NorESM1 model. The UC model simulates a bimodal rainfall and runoff system with a dry period during the rainy season in July to September. Although the model was forced by bias-correction into a completely different system, by pushing the dry season into a rainy season, the projections seem not anywhere near as disrupted as the IPSL simulation. Hence, the NorESM1 results do not support the assumption that strong bias-correction necessarily results in unexpected behaviour in future periods. Looking at the change of average peak magnitudes between UC and BC ESM simulations in the reference and future period, the change signals are in a similar order, except for simulations based on IPSL. They are also in the order of average peaks simulated with WFD input, compare with Figure 3.

Figure 11 shows that maximal discharge peaks simulated with RCM climate input is often much higher than average peaks simulated with WFD (~6000 m^3s^{-1}). Where only two UC RCMs simulate higher peaks in the reference period (EC-EARTH-Hirham5 and EC-EARTH-RCA4), five BC RCM simulate peaks higher than 7000 m^3s^{-1}. Looking at projected peaks in the period 2030–2059 (RCP 8.5) shows that nine out of ten BC RCM-driven and five UC RCM simulations simulate peaks that are higher than 7000 m^3s^{-1}. The projected changes of peak discharge magnitudes between UC and BC RCMs is significantly higher in BC simulations in 50% of the models. This is not surprising, because bias-correction of RCMs led to significant overestimation of high flows already in the reference period, as was discussed in Section 4.2.3. This behaviour is exaggerated in future periods.

4.5 Selected ensemble

Table 1 summarises the performance criteria for all UC and BC simulations using R^2, $PBIAS$, deviations from FDC values, and the change rate. The seasonality criterion $R^2 > 0.85$ was achieved by all simulations except the one based on UC NorESM. Seven out of 30 simulations failed to represent the volumetric deviation criterion $PBIAS \pm 30\%$. Concerning the FDC criteria, 12 simulations passed the NED test, seven simulations the high flow criterion and only one simulation the low flow criterion. The column *pre* (pre-selection) shows whether a model fulfilled the criteria in the first three columns. Those models might be chosen for a qualitative impact assessment. However, four models that passed the pre-selection criteria were omitted from the selected model ensemble because they project very high changes in average annual discharges (column *Change*). Sometimes both the UC and BC simulations were judged to be suitable. In order not to overweight the results of one model, only the better simulation (UC or BC) was selected into the final model ensemble and is denoted in column *final*. The latter column indicates that ten out of 30 simulations passed all performance criteria and thus become members of the selected model ensemble. This ensemble consists of four BC ESMs, four BC RCMs, and two UC RCMs.

4.6 Climate impacts on discharges

In this section, the similarities and differences of projected climate change impacts on Blue Nile discharges at gauge El Diem are discussed. Considered are the two UC and BC ESM and RCM ensembles and the selected model ensemble (see Table 1, column *final*). In Figures 12 and 13 and S8 to S11, each model simulation is represented by a semi-transparent polygon where blueish colours indicate increase and reddish colours decrease in monthly discharges. The more saturated the colour the more models project the same rate of change. The figures show monthly changes relative to average annual discharges in the reference period. This method was chosen in order not to overemphasise large relative changes in dry periods which are not significant compared to annual discharges.

Table 2 shows the total range of changes in average annual discharges projected by the multi-model means of UC and BC ESMs and RCMs and the selected model ensembles. In the near future (2030–2059) in both RCPs, the range of UC models is between 7.4% and 19%, the range of BC models between 11.3% and 27.7%, and the range of the selected ensemble between 5.8% and 11.3%. In the far future (2070–2099) considering both RCPs, the range of UC models is between 7.5% and 21.6%, the range of BC models between 20.3% and 56.7%, and the range of the selected ensemble between 8.4% and 13.2%. Following conclusions summarise the projected changes of average annual discharges more specifically:

- All ensembles in all RCPs and future periods have in common that they all project an increase of average annual discharges. An exception is the selected model ensemble of the UC ESMs under RCP 4.5 (2030–2059) which projects a decrease of -0.4% (Fig. S8a).

- The multi-model means of both UC and BC RCM ensembles (all models) project usually higher increase of average annual discharges than the ESM ensembles, except under RCP 8.5 (2070–2099), see Figures S9 d) and S11 d).

- The multi-model means of BC simulations (both RCPs and periods) always project higher increases in average annual discharges than the UC multi-model means.

- The magnitude of change signals projected by selected models in the respective ensemble is always lower than the magnitude of the whole ensemble. This is mainly caused by the fact that models projecting changes of $> \pm 30\%$, between reference period and 2030–2059 under RCP 8.5, were omitted from the ensemble of selected models.

- A noticeable difference between the UC RCM and ESM ensembles is that projected average annual discharges in the far future are lower (RCMs) and higher (ESMs) than in the near future.

General findings concerning changes in seasonality:

- There is a trend of decreasing discharges at the end of the dry season projected by all ensembles in both RCPs and periods. The period indicating a drying trend projected by the ESM ensemble tends to be longer and starts a bit earlier (June/July to August) than the trend projected by RCMs (only July).

– There is a trend of increasing discharges during the rainy season projected by all ensembles in both RCPs and periods. The period indicating higher discharges starts earlier in the RCM ensembles (August to November) than in the ESM ensembles (September to November).

– Both ensembles agree that there is almost no change projected in the dry period between December and May.

5 Discussion and conclusions

Are we using the right fuel to drive hydrological models? What are the likely impacts of climate change on future discharges in the UBN and is there a strong agreement of projected trends? In how far does bias-correction influence the results and can we trust models that required strong correction? These questions, posed in the introduction, are discussed in the following.

The majority ($\geq$80%) of the 15 climate models used in this study agree that average annual discharges in the UBN are likely to increase in future. The models project a trend towards decreasing discharges at the end of the dry period (June and July) and an increase during the rainy season (August to November). Due to the usage of different climate model ensembles, downscaling approaches, study areas within the UBN, and periods of analysis, a direct comparison with other studies is difficult but clearly reveals that the selection of climate models is predominantly influencing the results and conclusions made. Setegn et al. (2011) found for instance that the CMIP3 GCMs they used to investigate climate impacts on discharges in the Lake Tana catchment (Blue Nile headwaters) project decreasing trends but they also state that "*...it seems that, by chance, the nine GCMs used in this study are those that show a precipitation decrease...*". On the other hand Dile et al. (2013) conclude that discharges may increase by up to 135% in the same region. Taking the, sometimes contradicting, results of recent studies into account (Teklesadik et al., 2017; Dile et al., 2013; Mengistu and Sorteberg, 2012; McCartney and Menker Girma, 2012; Setegn et al., 2011; Conway and Schipper, 2011; Diro et al., 2011; Elshamy et al., 2009), one can conclude that climate impacts in the UBN are uncertain but there is a bias towards a wetter future. The findings of this study, using most recent global and regional climate models as well as precipitation projections of the entire CMIP5 ensemble, are underlining the latter statement.

Apart from discussing whether the future in the UBN will become generally wetter or drier, decisions with regard to adaptation of land and water management to changing climatic conditions requires not only information on qualitative but also accurate seasonal quantitative changes. The value of using uncorrected climate simulations to answer those questions is, due to the lack of spatio-temporal accuracy and the lack of statistically representing observed weather characteristics, usually rather limited. Bias-correction of climate simulations is an attempt to overcome at least some of these deficiencies.

The reference dataset used to bias-correct climate models and to calibrate and validate the hydrological model is another source of uncertainty. WFD were used in this study because bias-correction on ESMs, provided by ISIMIP, was performed on the basis of this dataset. Moreover, WFD provide a sound basis as climate input, particularly in data scarce regions, as was shown in various studies (Vetter et al., 2015; Aich et al., 2014; Liersch et al., 2013). The usage of a different reference dataset would certainly require different calibration parameter settings and correction factors but would probably not impact the change signals. The most important issue in this connection is the consistency in using the same reference for calibration, validation, and bias-correction.

As was shown in this study, monthly medians and average annual precipitation amounts of UC ESM and RCM simulations deviate sometimes strongly from reference climate. Although bias-correction improved the performance of average climate conditions, the range of monthly precipitation amounts increased critically in several models, producing some extreme outliers in both ensembles. This phenomenon was particularly observed in simulations where deviations of monthly medians between UC simulations and WFD was rather large in the reference period. Average daily precipitation and the number of rainy days were considerably improved by bias-correction, but 13 out of 15 BC models overestimate daily precipitation maxima and many of them significantly. Hence, the bias-correction methods applied to ESMs and RCMs in this study could be considered as only partly successful. While achieving significant improvement in terms of average daily, monthly, and annual precipitation characteristics, increasing variability of precipitation amounts and therefore under and overestimation of extremes was the result in many simulations.

This phenomenon is problematic for impact studies and the application of hydrological models, particularly if changes of extreme values are the subject of investigation. Large overestimation of precipitation on some days or in some months for instance, which are balanced by dry months in the long term, can lead to large amounts of excess water that may be simulated almost entirely as surface runoff by the hydrological model. Therefore, it is reasonable to use hydrological performance indicators to evaluate the suitability of climate simulations, particularly for quantitative impact studies, and to create a subset of models for the impact assessment. Another way to deal with low performance in the simulation of extremes in impact studies is to analyse changes in return periods of extreme events (Hattermann et al., 2016).

Due to the fact that discharge simulations, based on climate simulations, cannot be compared to observed discharges on a real-time daily, monthly, or annual basis, the methods to evaluate discharge performance are limited. In this study, the annual cycle (daily time series averaged over the simulation period) was characterised by R^2 and $PBIAS$, where R^2 was a measure for seasonality and $PBIAS$ for volumetric deviations. Flow Duration Curves (FDCs) were used to characterise the distribution of average flow conditions, high and low flows as well as their extremes by using the whole time series of daily discharge simulations. Unsurprisingly, discharge simulations show similar deficiencies as precipitation simulations. Using bias-corrected climate simulations improved the performance of non-extreme discharges (NED) significantly but, with few exceptions, the performance of high and low flows was not improved, in fact has worsened in most of the simulations. Many BC discharge simulations tend to exaggerate high (overestimation) and low flows (underestimation). Comparing peak discharges using UC and BC climate input, for instance, showed a tremendous increase in some BC simulations although average monthly precipitation patterns of BC models achieved a much better fit than their UC counterparts. Moreover, the multi-model means of BC simulations (both RCPs and periods) always project higher increases in average annual discharges than the UC multi-model means. However, a hydrological impact study in the Danube River basin showed in turn that relative changes of average monthly discharges projected by using UC and BC climate models are overall comparable (Stagl and Hattermann, 2015).

Knowing these limitations, one should carefully consider the model's suitability and the purpose it is being used for. An impact study focusing on relative changes of future water availability may have lower requirements in terms of model accuracy than a study with the aim to investigate future extremes, such as floods and droughts or a study addressing land and

water management issues including irrigation and/or reservoir operations. Whenever complex water management is involved, bias-correction is often unavoidable, because the simulation of reservoir and irrigation operations require rather accurate hydrological input. However, to simply trust in climate input only because it was bias-corrected would be naive. Therefore, the question of model selection is valid. Why should one use or trust models to assess changes in seasonal patterns, for instance, that are not representing those patterns in the past or use a model to investigate future flood risk that completely fails to represent rainfall extremes? Again, bias-correction may help to overcome some quality issues but it was also found in this study that improving climate simulations in the reference period does not guarantee higher quality or reliability in simulating future periods. On the contrary, the greater the necessity to correct a particular model, the higher the risk that BC simulations will show unexpected behaviour in future periods, where exceptions confirm the rule. Examples confirming this assumption are the following models: IPSL, CanESM2-RCA4, CNRM-CM5-RCA4, and MIROC-RCA4. However, the NorESM1 model is an exception here, because the BC simulation does not show extreme changes in future periods although strong bias-correction was necessary in some months to force the model from a bimodal into a unimodal rainfall regime. It should be emphasised that the analysis of climate model performance in this study is only valid for the region of the UBN. It does not imply that a model which performed poorly in this study area is generally performing "poorly" in other regions, too.

The authors of this study conclude that a purpose-driven selection of a climate model subset is a reasonable approach, particularly in a regional context. To identify "good performing" models, the selection process should include an analysis of climate inputs, seasonal discharge patterns, volumetric deviations, daily dynamics (FDCs), and an assessment of the magnitude of projected future changes. It is also worth mentioning that the thresholds defined to evaluate model performance have a subjective component and are based on statistical parameters, graphical data interpretation, and modelling expertise. If the thresholds would have been set more critically in this study, almost no climate model would have passed the evaluation process successfully. The rather weak thresholds were a compromise and reveal the fact that the performance of many climate models is still far beyond being adequate for applied quantitative impact studies. This statement includes bias-corrected simulations and implies that the ability of bias-correction can, depending on the approach, be rather limited and is thus not per se necessarily improving the reliability. In another river basin with different characteristics, e.g. with a nival regime or a bimodal rainfall regime, the performance criteria and their thresholds may have been defined differently. Hence, the model selection method can be applied to other river basins but it is always necessary to consider region-specific characteristics that may require the introduction of new criteria adapted to the situation at hand. However, model selection for regional impact studies is only a reasonable, justifiable, and recommended approach if the uncertainties of the selected ensemble are communicated within the context of the whole model ensemble.

This study demonstrated that neither the trend-preserving method applied to the five ESMs nor the harmonic-based method used to bias-correct the ten RCMs was able to generate fully satisfactory climate inputs for a regional hydrological impact study with high demands in terms of quantitative accuracy. Hence, further research is required to improve regional climate simulations and/or to investigate alternative correction methods or approaches to make available climate simulations meaningful for application-oriented regional studies. Currently, the most promising solutions seem to be sophisticated delta-change methods, as suggested by Anandhi et al. (2011), Bosshard et al. (2011), and Chiew et al. (2009)

Acknowledgements. This research was funded by the German Federal Foreign Office and supported by the Ethiopian Environmental Protection Authority and the German Embassy in Addis Ababa.

References

Abdo, K. S., Fiseha, B. M., Rientjes, T. H. M., Gieske, A. S. M., and Haile, A. T.: Assessment of climate change impacts on the hydrology of Gilgel Abay catchment in Lake Tana basin, Ethiopia, Hydrological Processes, 23, 3661–3669, doi:10.1002/hyp.7363, 2009.

Addor, N. and Seibert, J.: Bias correction for hydrological impact studies - beyond the daily perspective, Hydrological Processes, 28, 4823–4828, doi:10.1002/hyp.10238, 2014.

Aich, V., Liersch, S., Vetter, T., Huang, S., Tecklenburg, J., Hoffmann, P., Koch, H., Fournet, S., Krysanova, V., Müller, E. N., and Hattermann, F. F.: Comparing impacts of climate change on streamflow in four large African river basins, Hydrology and Earth System Sciences, 18, 1305–1321, doi:10.5194/hess-18-1305-2014, 2014.

Anandhi, A., Frei, A., Pierson, D. C., Schneiderman, E. M., Zion, M. S., Lounsbury, D., and Matonse, A. H.: Examination of change factor methodologies for climate change impact assessment, Water Resour Res, 47, doi:10.1029/2010WR009104, 2011.

Arnold, J., Allen, P., and Bernhardt, G.: A comprehensive surface groundwater flow model, Journal of Hydrology, 142, 47–69, 1993.

Bartholomé, E. and Belward, A.: GLC2000: a new approach to global land cover mapping from Earth observation data, International Journal of Remote Sensing, 26, 1959–1977, doi:10.1080/01431160412331291297, 2005.

Berg, P., Feldmann, H., and Panitz, H.-J.: Bias correction of high resolution regional climate model data, Journal of Hydrology, 448–449, 80–92, doi:10.1016/j.jhydrol.2012.04.026, 2012.

Beyene, T., Lettenmaier, D., and Kabat, P.: Hydrologic impacts of climate change on the Nile River Basin: implications of the 2007 IPCC scenarios, Climatic Change, 100, 433–461, doi:10.1007/s10584-009-9693-0, 2010.

Bosshard, T., Kotlarski, S., Ewen, T., and Schär, C.: Spectral representation of the annual cycle in the climate change signal, Hydrology and Earth System Sciences, 15, 2777–2788, doi:10.5194/hess-15-2777-2011, 2011.

Bryan, E., Deressa, T. T., Gbetibouo, G. A., and Ringler, C.: Adaptation to climate change in Ethiopia and South Africa: options and constraints, Environmental Science & Policy, 12, 413–426, doi:10.1016/j.envsci.2008.11.002, special Issue: Food Security and Environmental Change Food Security and Environmental Change: Linking Science, Development and Policy for Adaptation, 2009.

Busby, J., Cook, K., Vizy, E., Smith, T., and Bekalo, M.: Identifying hot spots of security vulnerability associated with climate change in Africa, Climatic Change, 124, 717–731, doi:10.1007/s10584-014-1142-z, 2014.

Chiew, F. H. S., Teng, J., Vaze, J., Post, D. A., Perraud, J. M., Kirono, D. G. C., and Viney, N. R.: Estimating climate change impact on runoff across southeast Australia: Method, results, and implications of the modeling method, Water Resour Res, 45, doi:10.1029/2008WR007338, 2009.

Christensen, J. H., Boberg, F., Christensen, O. B., and Lucas-Picher, P.: On the need for bias correction of regional climate change projections of temperature and precipitation, Geophysical Research Letters, 35, doi:10.1029/2008GL035694, 2008.

Conway, D. and Hulme, M.: Recent fluctuations in precipitation and runoff over the Nile sub-basins and their impact on main Nile discharge, Climatic Change, 25, 127–151, doi:10.1007/BF01661202, 1993.

Conway, D. and Schipper, E. L. F.: Adaptation to climate change in Africa: Challenges and opportunities identified from Ethiopia, Global Environmental Change, 21, 227 – 237, doi:10.1016/j.gloenvcha.2010.07.013, 2011.

Deressa, T. T., Hassan, R. M., and Ringler, C.: Perception of and adaptation to climate change by farmers in the Nile basin of Ethiopia, The Journal of Agricultural Science, 149, 23–31, doi:10.1017/S0021859610000687, 2011.

Di Baldassarre, G., Elshamy, M., van Griensven, A., Soliman, E., Kigobe, M., Ndomba, P., Mutemi, J., Mutua, F., Moges, S., Xuan, Y., Solomatine, D., and Uhlenbrook, S.: Future hydrology and climate in the River Nile basin: a review, Hydrological Sciences Journal-Journal Des Sciences Hydrologiques, 56, 199–211, doi:10.1080/02626667.2011.557378, 2011.

Dile, Y. T., Berndtsson, R., and Setegn, S. G.: Hydrological Response to Climate Change for Gilgel Abay River, in the Lake Tana Basin - Upper Blue Nile Basin of Ethiopia, PLOS ONE, 8, doi:10.1371/journal.pone.0079296, 2013.

Diro, G. T., Grimes, D. I. F., Black, E., O'Neill, A., and Pardo-Iguzquiza, E.: Evaluation of reanalysis rainfall estimates over Ethiopia, International Journal of Climatology, 29, 67–78, doi:10.1002/joc.1699, 2009.

Diro, G. T., Toniazzo, T., and Shaffrey, L.: Ethiopian Rainfall in Climate Models, in: African Climate and Climate Change, edited by Williams, C. J. R. and Kniveton, D. R., vol. 43 of *Advances in Global Change Research*, pp. 51–69, Springer Netherlands, doi:10.1007/978-90-481-3842-5_3, 2011.

Dobler, A. and Ahrens, B.: Precipitation by a regional climate model and bias correction in Europe and South Asia, Meteor. Z., 17, 499–509, 2008.

Dobler, A., Yaoming, M., Sharma, N., Kienberger, S., and Ahrens, B.: Regional climate projections in two alpine river basins: Upper Danube and Upper Brahmaputra, Advances in Science and Research, 7, 11–20, doi:10.5194/asr-7-11-2011, 2011.

Dosio, A. and Paruolo, P.: Bias correction of the ENSEMBLES high-resolution climate change projections for use by impact models: Evaluation on the present climate, Journal of Geophysical Research: Atmospheres, 116, doi:10.1029/2011JD015934, 2011.

Elshamy, M., di Baldassarre, G., and van Griensven, A.: Characterizing Climate Model Uncertainty Using an Informal Bayesian Framework: Application to the River Nile, Journal of hydrologic engineering ASCE, 18, 582–589, doi:10.1061/(ASCE)HE.1943-5584, 2013.

Elshamy, M. E., Seierstad, I. A., and Sorteberg, A.: Impacts of climate change on Blue Nile flows using bias-corrected GCM scenarios, Hydrology and Earth System Sciences, 13, 551–565, doi:10.5194/hess-13-551-2009, 2009.

FAO, IIASA, ISRIC, ISSCAS, and JRC: Harmonized World Soil Database (version 1.1)., FAO, Rome, Italy and IIASA, Laxenburg, Austria, http://www.fao.org/nr/land/soils/harmonized-world-soil-database/en/, 2009.

Gebreluel, G.: Ethiopia's Grand Renaissance Dam: Ending Africa's Oldest Geopolitical Rivalry?, Wash Quart, 37, 25–37, doi:10.1080/0163660X.2014.926207, 2014.

Gudmundsson, L., Bremnes, J. B., Haugen, J. E., and Engen-Skaugen, T.: Technical Note: Downscaling RCM precipitation to the station scale using statistical transformations – a comparison of methods, HESS, 16, 3383–3390, doi:10.5194/hess-16-3383-2012, 2012.

Hagemann, S., Chen, C., Haerter, J. O., Heinke, J., Gerten, D., and Piani, C.: Impact of a Statistical Bias Correction on the Projected Hydrological Changes Obtained from Three GCMs and Two Hydrology Models, Journal of Hydrometeorology, 12, 556–578, doi:10.1175/2011JHM1336.1, 2011.

Hargreaves, G. and Samani, Z.: Reference crop evapotranspiration from temperature, Transaction of ASAE, 11, 96–99, 1985.

Hattermann, F. F., Huang, S., Burghoff, O., Hoffmann, P., and Kundzewicz, Z. W.: Brief Communication: An update of the article "Modelling flood damages under climate change conditions – a case study for Germany", Natural Hazards and Earth System Sciences, 16, 1617–1622, doi:10.5194/nhess-16-1617-2016, 2016.

Headey, D., Taffesse, A. S., and You, L.: Diversification and Development in Pastoralist Ethiopia, World Development, 56, 200–213, doi:10.1016/j.worlddev.2013.10.015, 2014.

Hempel, S., Frieler, K., Warszawski, L., Schewe, J., and Piontek, F.: A trend-preserving bias correction – the ISI-MIP approach, Earth System Dynamics Discussions, 4, 49–92, doi:10.5194/esdd-4-49-2013, 2013.

Ibrahim, A.: The Nile Basin Cooperative Framework Agreement: The Beginning of the End of Egyptian Hydro-Political Hegemony, Missouri Environmental Law and Policy Review, 18, 284–312, http://law.missouri.edu/melpr/recentpublications/Ibrahim.pdf, 2012.

IPCC: Climate Change 2013. The Physical Science Basis. Working Group I Contribution to the Fifth Assessment Report of the Intergovernmental Panel on Climate Change, Tech. rep., IPCC, http://www.ipcc.ch/report/ar5/wg1/, 2013.

Jarvis, A., Reuter, H., Nelson, A., and Guevara, E.: Hole-filled seamless SRTM data V4, International Centre for Tropical Agriculture (CIAT), http://srtm.csi.cgiar.org., 2008.

Jeuland, M. and Whittington, D.: Water resources planning under climate change: Assessing the robustness of real options for the Blue Nile, Water Resour Res, 50, 2086–2107, doi:10.1002/2013WR013705, 2014.

Kim, U., Kaluarachchi, J. J., and Smakhtin, V. U.: Climate Change Impacts on Hydrology and Water Resources of the Upper Blue Nile River Basin, Ethiopia, Research Report 126, IWMI, 2008.

King, A.: An Assessment of Reservoir Filling Policies under a Changing Climate for Ethiopias Grand Renaissance Dam, Ph.D. thesis, Drexel University, 2013.

Koch, H., Liersch, S., and Hattermann, F.: Integrating water resources management in eco-hydrological modelling, Water Science & Technology, 67, 1525–1533, doi:10.2166/wst.2013.022, 2013.

Krysanova, V., Meiner, A., Roosaare, J., and Vasilyev, A.: Simulation modelling of the coastal waters pollution from agricultural watershed, Ecological Modelling, 49, 7–29, 1989.

Krysanova, V., Hattermann, F., and Wechsung, F.: Development of the ecohydrological model SWIM for regional impact studies and vulnerability assessment, Hydrological Processes, 19, 763–783, doi:10.1002/hyp.5619, 2005.

Krysanova, V., Hattermann, F., Huang, S., Hesse, C., Vetter, T., Liersch, S., Koch, H., and Kundzewicz, Z. W.: Modelling climate and land use change impacts with SWIM: lessons learnt from multiple applications, Hydrological Sciences Journal, 60, 606–635, doi:10.1080/02626667.2014.925560, 2015.

Liersch, S., Cools, J., Kone, B., Koch, H., Diallo, M., Aich, V., Fournet, S., and Hattermann, F.: Vulnerability of food production in the Inner Niger Delta to water resources management under climate variability and change, Environmental Science and Policy, 34, 18–33, doi:10.1016/j.envsci.2012.10.014, 2013.

Liersch, S., Koch, H., and Hattermann, F. F.: Management Scenarios of the Grand Ethiopian Renaissance Dam and Their Impacts under Recent and Future Climates, Water, 9, doi:10.3390/w9100728, 2017.

Maraun, D., Wetterhall, F., Ireson, A. M., Chandler, R. E., Kendon, E. J., Widmann, M., Brienen, S., Rust, H. W., Sauter, T., Themeßl, M., Venema, V. K. C., Chun, K. P., Goodess, C. M., Jones, R. G., Onof, C., Vrac, M., and Thiele-Eich, I.: Precipitation downscaling under climate change: Recent developments to bridge the gap between dynamical models and the end user, Reviews of Geophysics, 48, doi:10.1029/2009RG000314, 2010.

McCartney, M. P. and Menker Girma, M.: Evaluating the downstream implications of planned water resource development in the Ethiopian portion of the Blue Nile River, Water International, 37, 362–379, doi:10.1080/02508060.2012.706384, 2012.

Megersa, B., Markemann, A., Angassa, A., Ogutu, J. O., Piepho, H.-P., and Zarate, A. V.: Impacts of climate change and variability on cattle production in southern Ethiopia: Perceptions and empirical evidence, Agricultural Systems, 130, 23–34, doi:10.1016/j.agsy.2014.06.002, 2014.

Meinshausen, M., Smith, S., Calvin, K., Daniel, J., Kainuma, M., Lamarque, J.-F., Matsumoto, K., Montzka, S., Raper, S., Riahi, K., Thomson, A., Velders, G., and Vuuren, D.: The RCP greenhouse gas concentrations and their extensions from 1765 to 2300, Climatic Change, 109, 213–241, doi:10.1007/s10584-011-0156-z, 2011.

Mengistu, D., Bewket, W., and Lal, R.: Recent spatiotemporal temperature and rainfall variability and trends over the Upper Blue Nile River Basin, Ethiopia, Int J Climatol, 34, 2278–2292, doi:10.1002/joc.3837, 2014.

Mengistu, D. T. and Sorteberg, A.: Sensitivity of SWAT simulated streamflow to climatic changes within the Eastern Nile River basin, HESS, 16, 391–407, doi:10.5194/hess-16-391-2012, 2012.

Moriasi, D. N., Arnold, J. G., Van Liew, M. W., Bingner, R. L., Harmel, R. D., and Veith, T. L.: Model evaluation guidelines for systematic quantification of accuracy in watershed simulations, Transactions of the ASABE, 50, 885–900, 2007.

Nash, J. and Sutcliffe, J.: River flow forecasting through conceptual models, Part 1 - a discussion of principles, Journal of Hydrology, 10, 282–290, doi:10.1016/0022-1694(70)90255-6, 1970.

Piani, C., Weedon, G., Best, M., Gomes, S., Viterbo, P., Hagemann, S., and Haerter, J.: Statistical bias correction of global simulated daily precipitation and temperature for the application of hydrological models, Journal of Hydrology, 395, 199–215, doi:10.1016/j.jhydrol.2010.10.024, 2010.

Pierce, D. W., Barnett, T. P., Santer, B. D., and Gleckler, P. J.: Selecting global climate models for regional climate change studies, PNAS, 106, 8441–8446, doi:10.1073/pnas.0900094106, 2009.

Rust, H. W., Kruschke, T., Dobler, A., Fischer, M., and Ulbrich, U.: Discontinuous daily Temperatures in the WATCH forcing data setes, J. Hydrometeor., 16, 465–472, doi:10.1175/JHM-D-14-0123.1, 2015.

Schmidli, J., Frei, C., and Vidale, P. L.: Downscaling from GCM precipitation: A benchmark for dynamical and statistical downscaling methods, International Journal of Climatology, 26, 679–689, doi:10.1002/joc.1287, 2006.

Setegn, S. G., Rayner, D., Melesse, A. M., Dargahi, B., and Srinivasan, R.: Impact of climate change on the hydroclimatology of Lake Tana Basin, Ethiopia, Water Resour Res, 47, doi:10.1029/2010WR009248, 2011.

Simane, B., Zaitchik, B. F., and Mesfin, D.: Building Climate Resilience in the Blue Nile/Abay Highlands: A Framework for Action, Int J OF Environ Res Public Health, 9, 610–631, doi:10.3390/ijerph9020610, 2012.

Smakhtin, V.: Estimating daily flow duration curves from monthly streamflow data, Water SA, 26, 13–18, http://www.wrc.org.za, 2000.

Soliman, E. S., Sayed, M. A. A., and Jeuland, M.: Impact Assessment of Future Climate Change for the Blue Nile Basin, Using a RCM Nested in a GCM, Nile Basin Water Engineering Scientific Magazine, 2, 15–30, 2009.

Stagl, J. C. and Hattermann, F. F.: Impacts of Climate Change on the Hydrological Regime of the Danube River and Its Tributaries Using an Ensemble of Climate Scenarios, Water, 7, 6139–6172, doi:10.3390/w7116139, 2015.

Sutcliffe, J. and Parks, Y.: The Hydrology of the Nile, no. 5 in Special Publication, IAHS, Institute of Hydrology, Wallingford, Oxfordshire OX10 8BB, UK, iSBN 1-910502-75-9, 1999.

Taye, M. T. and Willems, P.: Temporal variability of hydroclimatic extremes in the Blue Nile basin, Water Resour Res, 48, doi:10.1029/2011WR011466, 2012.

Taye, M. T., Willems, P., and Block, P.: Implications of climate change on hydrological extremes in the Blue Nile basin: A review, Journal of Hydrology: Regional Studies, 4, Part B, 280–293, doi:10.1016/j.ejrh.2015.07.001, 2015.

Taylor, K. E.: Summarizing multiple aspects of model performance in a single diagram, Journal of Geophysical Research: Atmospheres, 106, 7183–7192, doi:10.1029/2000JD900719, 2001.

Teklesadik, A. D., Alemayehu, T., van Griensven, A., Kumar, R., Liersch, S., Eisner, S., Tecklenburg, J., Ewunte, S., and Wang, X.: Inter-model comparison of hydrological impacts of climate change on the Upper Blue Nile basin using ensemble of hydrological models and global climate models, Climatic Change, 141, 517–532, doi:10.1007/s10584-017-1913-4, 2017.

Teutschbein, C. and Seibert, J.: Regional Climate Models for Hydrological Impact Studies at the Catchment Scale: A Review of Recent Modeling Strategies, Geography Compass, 4, 834–860, doi:10.1111/j.1749-8198.2010.00357.x, 2010.

Teutschbein, C. and Seibert, J.: Bias correction of regional climate model simulations for hydrological climate-change impact studies: Review and evaluation of different methods, Journal of Hydrology, 456-457, 12–29, doi:10.1016/j.jhydrol.2012.05.052, 2012.

Uppala, S. M., KÅllberg, P. W., Simmons, A. J., and et al.: The ERA-40 re-analysis, Quarterly Journal of the Royal Meteorological Society, 131, 2961–3012, doi:10.1256/qj.04.176, 2005.

van Vuuren, D., Edmonds, J., Kainuma, M., Riahi, K., Thomson, A., Hibbard, K., Hurtt, G., Kram, T., Krey, V., Lamarque, J.-F., Masui, T., Meinshausen, M., Nakicenovic, N., Smith, S., and Rose, S.: The representative concentration pathways: an overview, Climatic Change, 109, 5–31, doi:10.1007/s10584-011-0148-z, 2011.

Vetter, T., Huang, S., Aich, V., Yang, T., Wang, X., Krysanova, V., and Hattermann, F.: Multi-model climate impact assessment and intercomparison for three large-scale river basins on three continents, Earth System Dynamics, 6, 17–43, doi:10.5194/esd-6-17-2015, 2015.

Vrac, M. and Friederichs, P.: Multivariate—intervariable, spatial, and temporal—bias correction, J. Climate, 28, 218–237, 2015.

Warszawski, L., Frieler, K., Huber, V., Piontek, F., Serdeczny, O., and Schewe, J.: The Inter-Sectoral Impact Model Intercomparison Project (ISI–MIP): Project framework, Proceedings of the National Academy of Sciences, 111, 3228–3232, doi:10.1073/pnas.1312330110, 2014.

Weedon, G. P., Gomes, S., Viterbo, P., Shuttleworth, W. J., Blyth, E., Österle, H., Adam, J. C., Bellouin, N., Boucher, O., and Best, M.: Creation of the WATCH Forcing Data and its use to assess global and regional reference crop evaporation over land during the twentieth century., Journal of Hydrometeorology, p. 110531121709055, doi:10.1175/2011JHM1369.1, 2011.

Wilks, D. S.: Statistical methods in the atmospheric sciences, Academic Press, San Diego, CA, 3rd edn., 2011.

Yee, T. W.: Vector Generalized Linear and Additive Models: With an Implementation in R, Springer, 2015.

Zaitchik, B. F., Simane, B., Habib, S., Anderson, M. C., Ozdogan, M., and Foltz, J. D.: Building Climate Resilience in the Blue Nile/Abay Highlands: A Role for Earth System Sciences, Int J Environ Res Public Health, 9, 435–461, doi:10.3390/ijerph9020435, 2012.

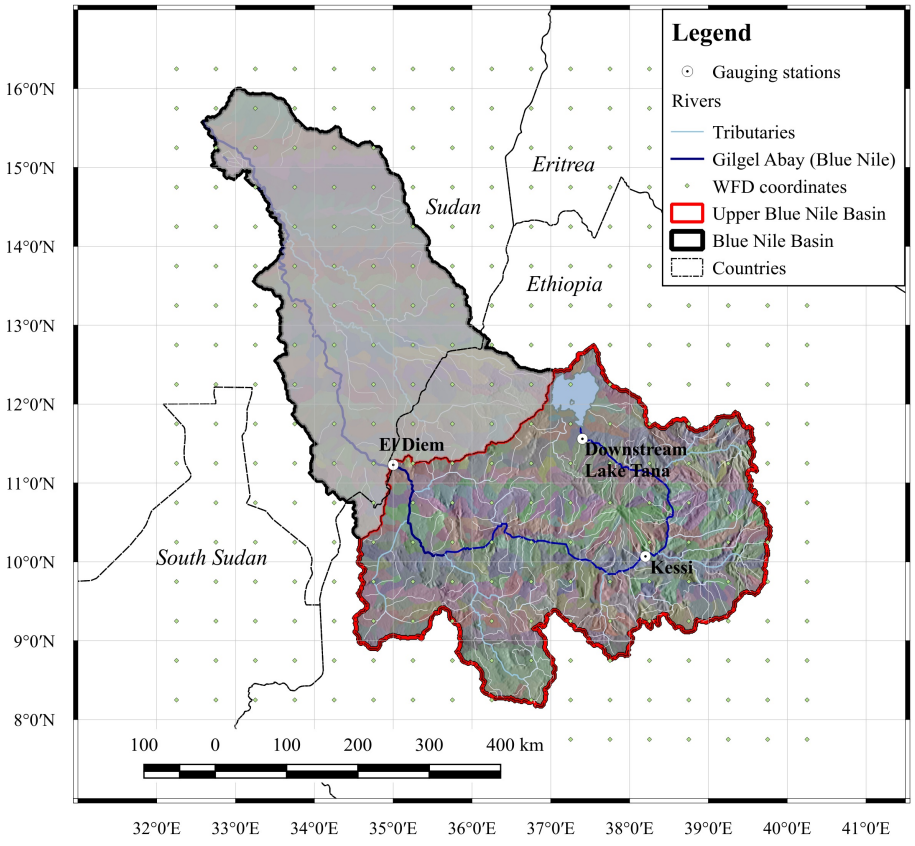

Figure 1. Map of the Blue Nile River basin. The Upper Blue Nile (UBN) catchment (172,000 km^2) is enclosed by the red line. The three gauges used for model calibration and validation are represented by white circles.

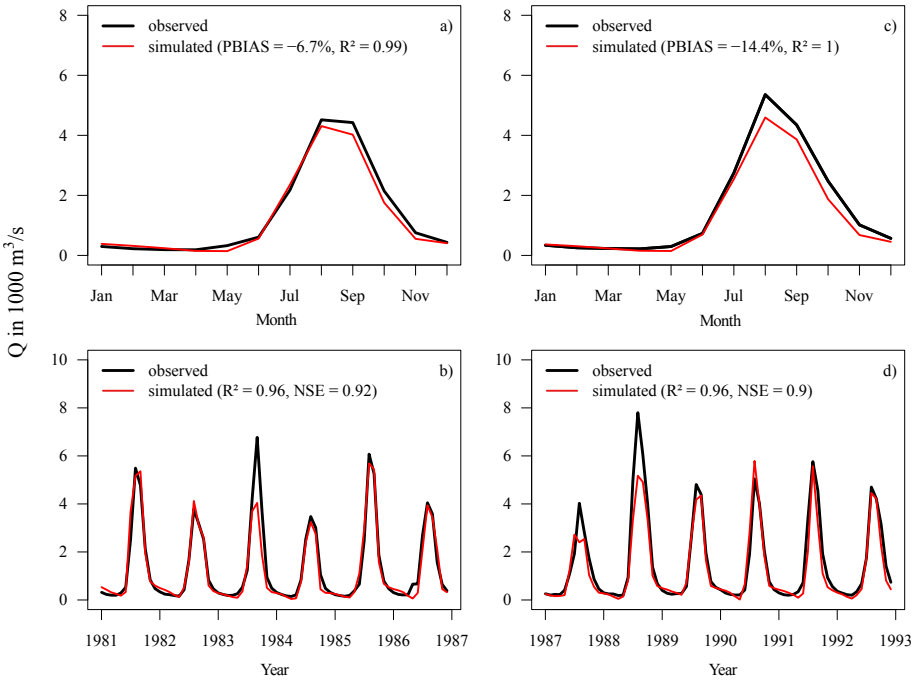

Figure 2. Simulated discharges for calibration (a and b) and validation (c and d) periods at gauge El Diem (Sudan Border) using WATCH Forcing Data (WFD). The annual cycle is shown in the top row and average monthly discharges in the bottom row.

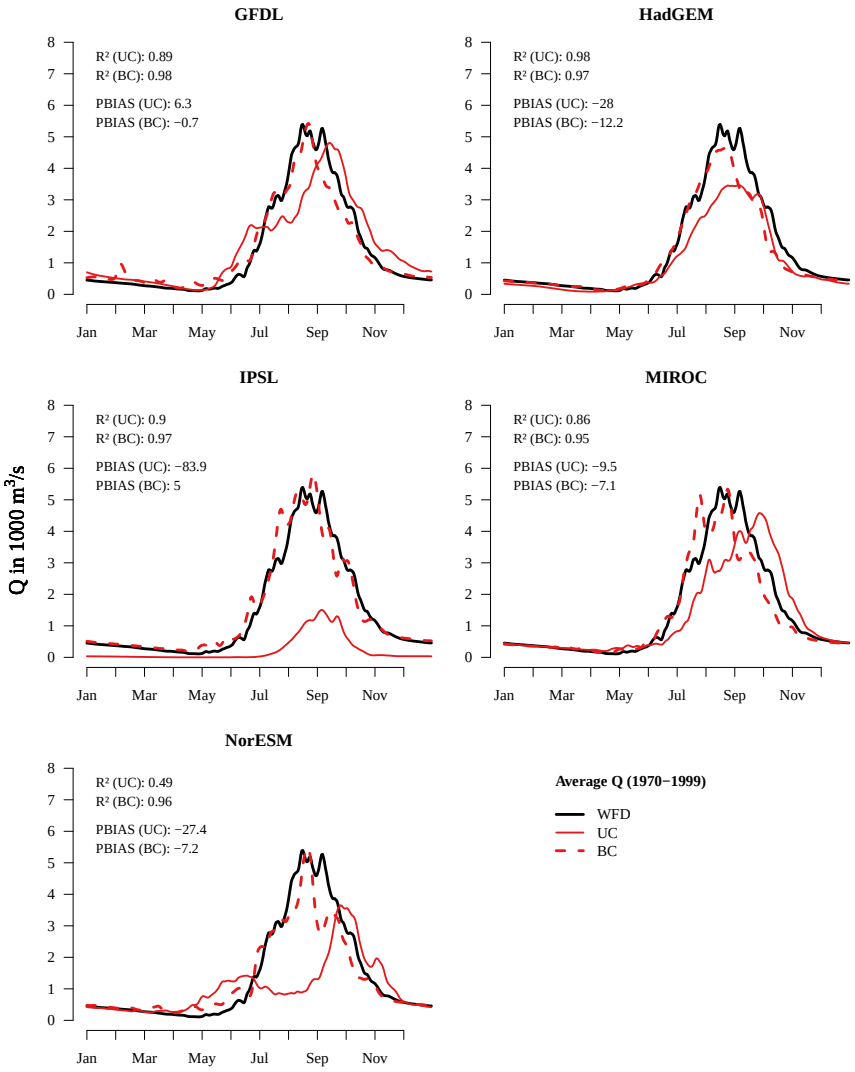

Figure 3. Annual cycle of average daily uncorrected (UC) and bias-corrected (BC) simulated discharges at gauge El Diem using Earth System Model input and WATCH Forcing Data (WFD) in the reference period (1970-1999).

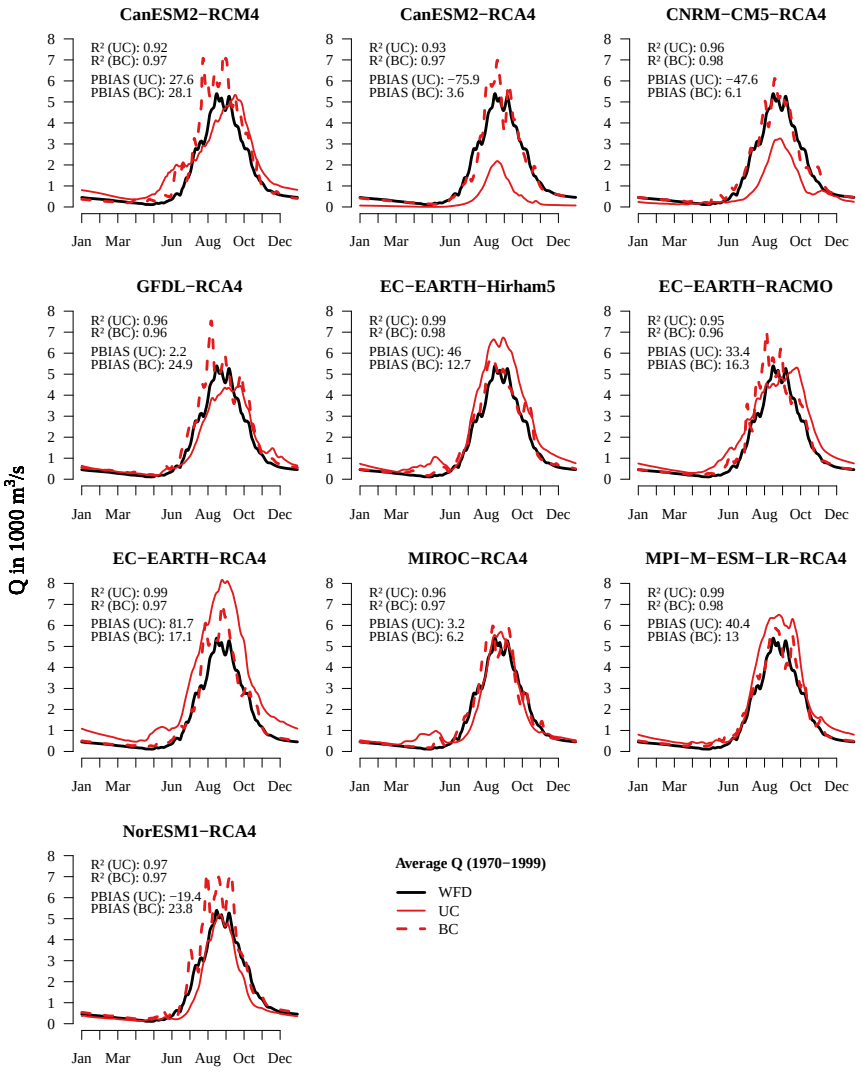

Figure 4. Annual cycle of average daily uncorrected (UC) and bias-corrected (BC) simulated discharges at gauge El Diem using Regional Climate Model input and WATCH Forcing Data (WFD) in the reference period (1970-1999).

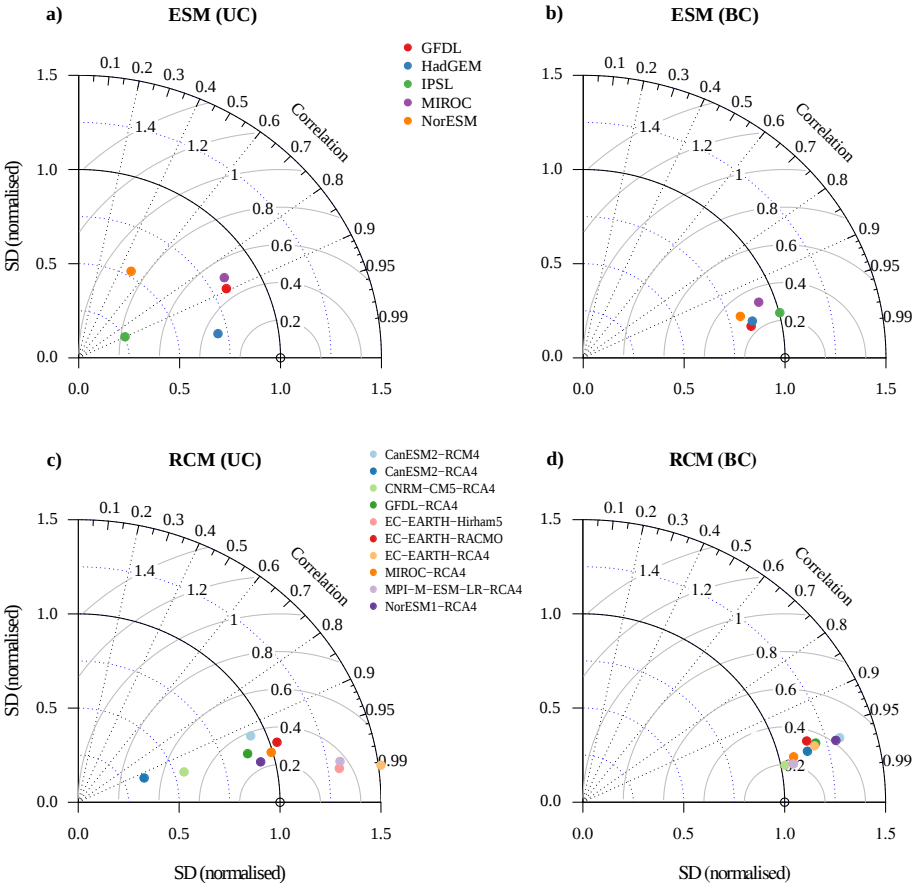

Figure 5. Taylor diagram of average daily discharges at gauge El Diem in the reference period (1970-1999). It shows R^2, standard deviation (SD) normalised by SD_{ref}, and normalised SD_D of discrepancies for Earth System Model (ESM) input in the top row and Regional Climate Model (RCM) input in the bottom row.

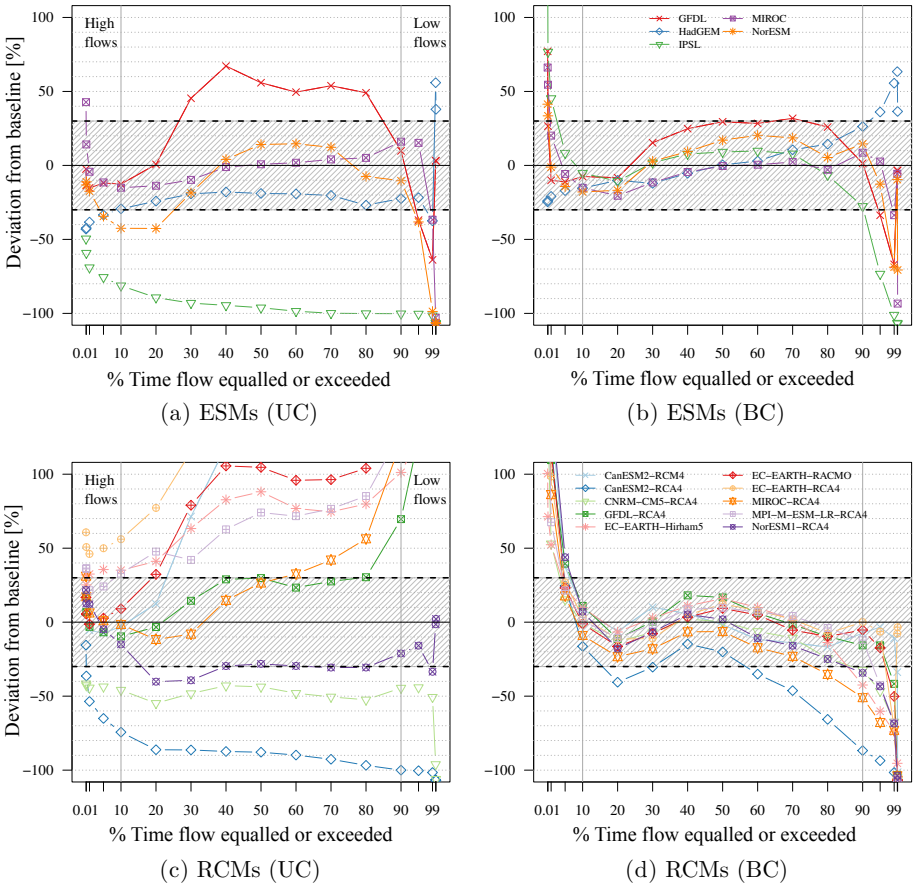

Figure 6. Relative deviations of FDCs from baseline discharge simulation at gauge El Diem using WATCH Forcing Data (WFD) in the reference period (1970-1999). Simulations based on uncorrected (UC) and bias-corrected (BC) Earth System Model (ESM) input in the top row and Regional Climate Model (RCM) input in the bottom row.

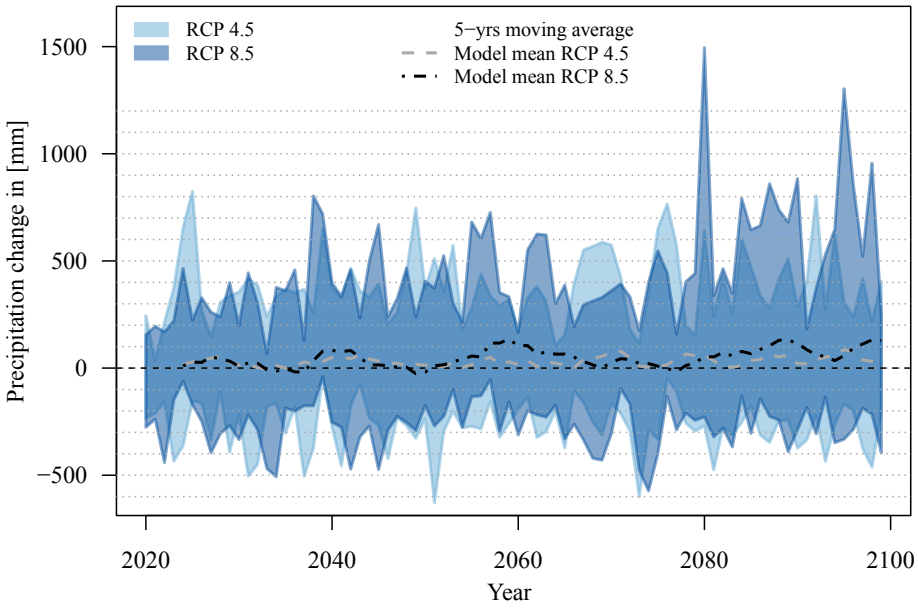

Figure 7. Anomalies of annual precipitation amounts relative to the reference period (1970-1999). Range of selected model ensemble.

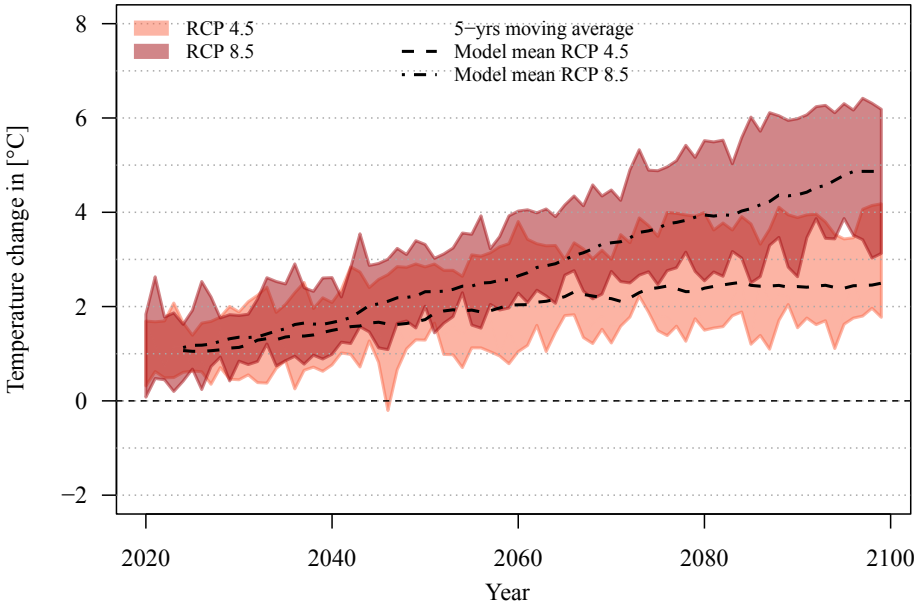

Figure 8. Anomalies of average annual mean air temperature relative to the reference period (1970-1999). Range of selected model ensemble.

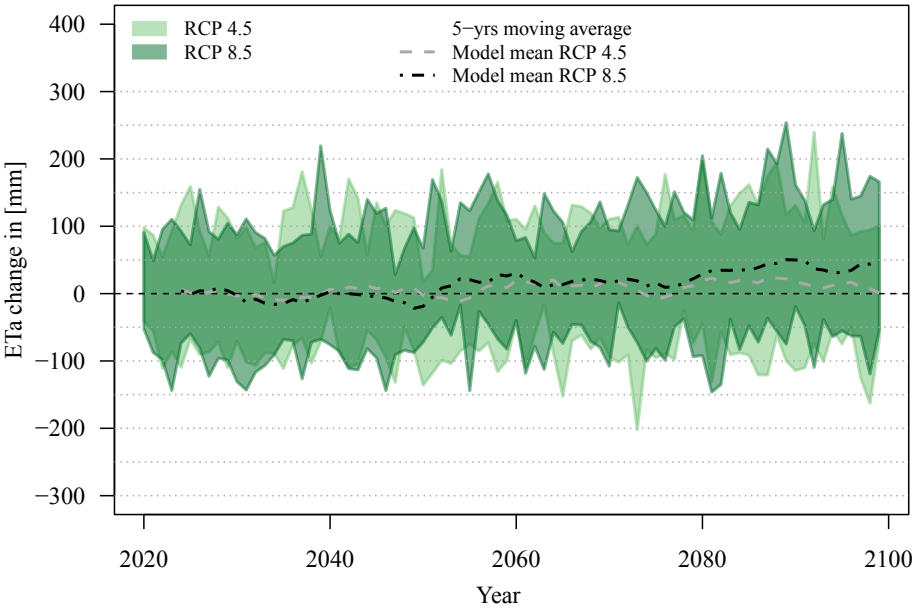

Figure 9. Anomalies of annual actual evapotranspiration amounts relative to the reference period (1970-1999). Range of selected model ensemble.

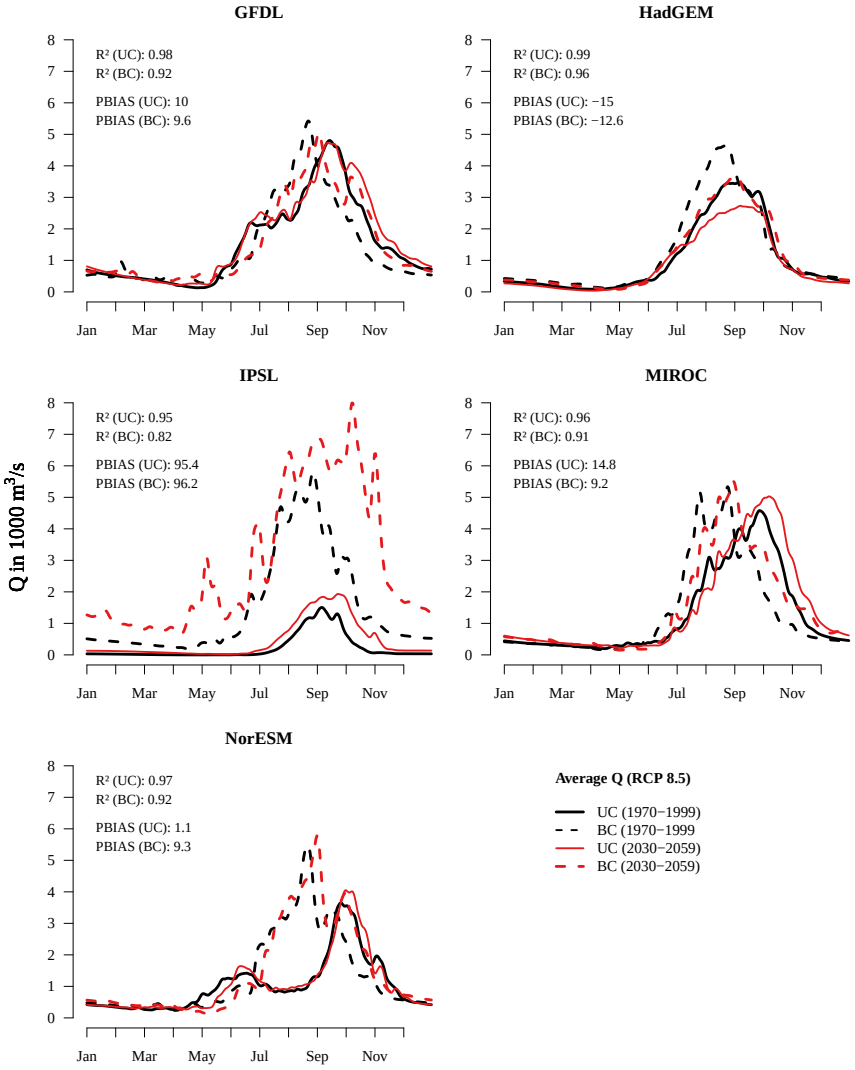

Figure 10. Changes of average daily discharges at gauge El Diem based on uncorrected (UC) and bias-corrected (BC) Earth System Models (ESM) input in the period (2030-2059) under RCP 8.5 relative to the models' reference period (1970-1999). R^2 and PBIAS values are computed to show the differences between projection period and reference period.

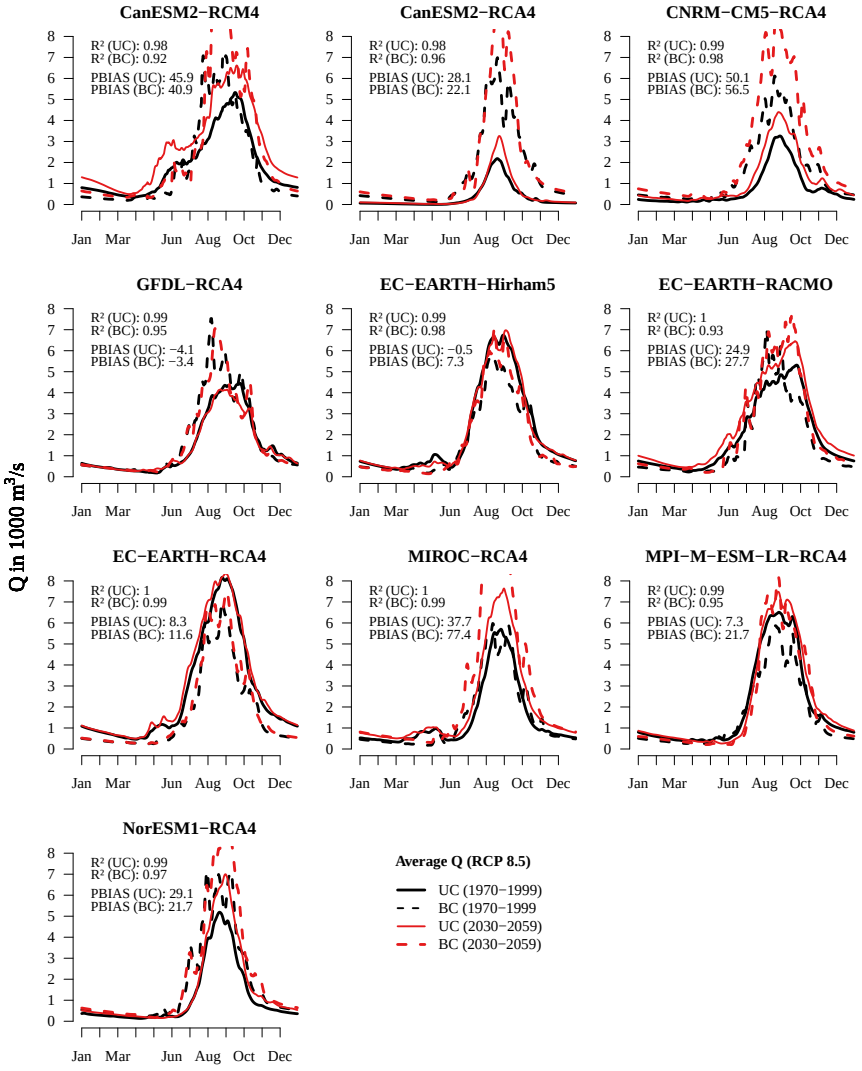

Figure 11. Changes of average daily discharges at gauge El Diem based on uncorrected (UC) and bias-corrected (BC) Regional Climate Model (RCM) input in the period (2030-2059) under RCP 8.5 relative to the models' reference period (1970-1999). R^2 and PBIAS values are computed to show the differences between projection period and reference period.

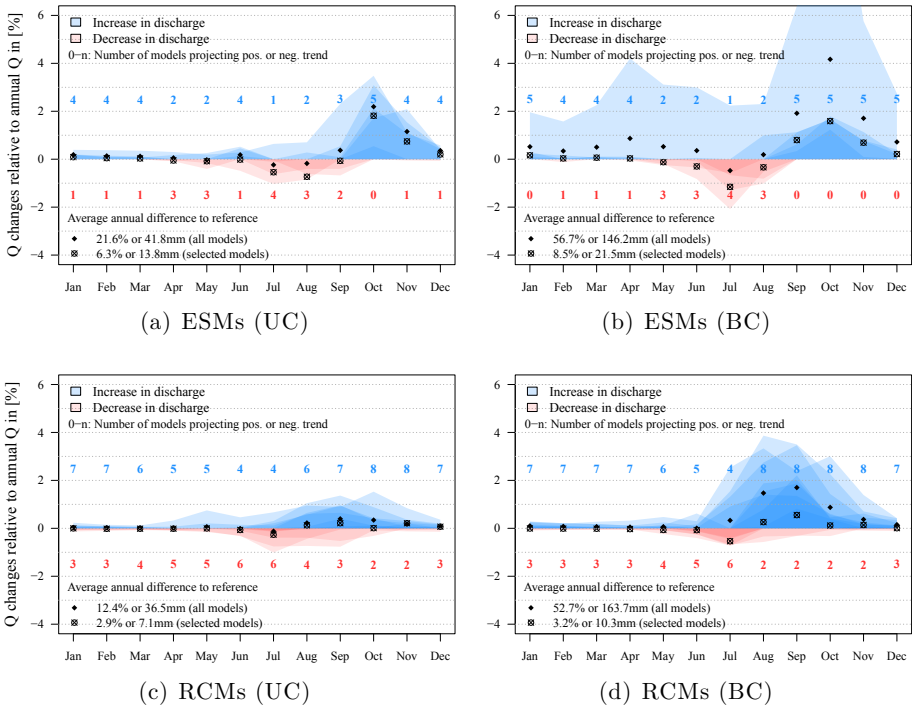

Figure 12. Monthly discharge changes of uncorrected (UC) and bias-corrected (BC) Earth System Model (ESM) and Regional Climate Model (RCM) simulations in [%] under RCP 8.5 (2070-2099). Monthly changes are relative to average annual discharge in the reference period (1970-1999) at gauge El Diem.

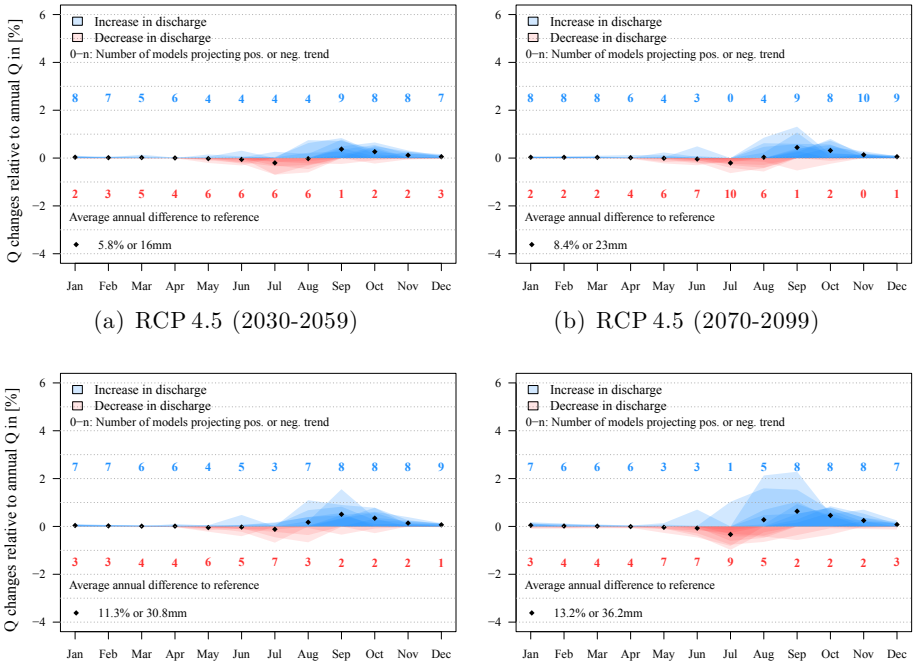

(a) RCP 4.5 (2030-2059) (b) RCP 4.5 (2070-2099)

(c) RCP 8.5 (2030-2059) (d) RCP 8.5 (2070-2099)

Figure 13. Monthly discharge changes of the selected model ensemble (10 models) relative to average annual discharge in the reference period (1970-1999) at gauge El Diem.

Table 1. Selection of uncorrected (UC) and bias-corrected (BC) Earth System Models (ESM) and Regional Climate Models (RCM)

	R^2	$PBIAS$	FDC $\pm 30\%$			Change	Selection	
Climate model	> 0.85	$\pm 30\%$	NED	HF	LF	$\pm 30\%$	pre	final
UC GFDL	x	x	–	x	–	x	–	–
BC GFDL	x	x	x	–	–	x	x	x
UC HadGEM	x	x	x	–	–	x	x	–
BC HadGEM	x	x	x	x	–	x	x	x
UC IPSL	x	–	–	–	–	–	–	–
BC IPSL	x	x	x	–	–	–	x	–
UC MIROC	x	x	x	~	–	x	x	–
BC MIROC	x	x	x	–	–	x	x	x
UC NorESM	–	x	~	~	–	x	–	–
BC NorESM	x	x	x	–	–	x	x	x
UC CanESM2/RCM4	x	x	–	x	–	–	–	–
BC CanESM2/RCM4	x	x	x	–	–	–	x	–
UC CanESM2/RCA4	x	–	–	–	–	x	–	–
BC CanESM2/RCA4	x	x	–	–	–	x	–	–
UC CNRM-CM5/RCA4	x	–	–	–	–	–	–	–
BC CNRM-CM5/RCA4	x	x	x	–	–	–	x	–
UC GFDL/RCA4	x	x	x	x	–	x	x	x
BC GFDL/RCA4	x	x	x	–	–	x	x	–
UC EC-EARTH/Hirham	x	–	–	~	–	x	–	–
BC EC-EARTH/Hirham	x	x	x	–	–	x	x	x
UC EC-EARTH/RACMO	x	–	–	x	–	x	–	–
BC EC-EARTH/RACMO	x	x	x	–	–	x	x	x
UC EC-EARTH/RCA4	x	–	–	–	–	x	–	–
BC EC-EARTH/RCA4	x	x	x	–	–	x	x	x
UC MIROC5/RCA4	x	x	–	x	–	–	–	–
BC MIROC5/RCA4	x	x	~	–	–	–	x	–
UC MPI-M-ESM-LR/RCA4	x	–	–	–	–	x	–	–
BC MPI-M-ESM-LR/RCA4	x	x	x	–	–	x	x	x
UC NorESM1/RCA4	x	x	~	x	x	x	x	x
BC NorESM1/RCA4	x	x	–	–	–	x	–	–

"x" = criterion achieved; "~" = criterion almost achieved; "–" = criterion not achieved

"HF" = high flows ($\leq Q_{10}$); "LF" = low flows ($\geq Q_{90}$)

"Change ± 30" = volumetric change between reference period and RCP 8.5 in 2030-2059

"pre" = pre-selection; "final" = models selected into the final ensemble

Table 2. Projected changes in average annual discharges relative to 1970-1999 in [%]

	RCP 4.5		RCP 8.5	
Model ensemble	2030-2059	2070-2099	2030-2059	2070-2099
UC ESMs	7.4	7.5	8.2	21.6
UC RCMs	18.5	14.2	19.0	12.4
BC ESMs	11.3	20.3	24.5	56.7
BC RCMs	23.5	22.3	27.7	52.7
Selected	5.8	8.4	11.3	13.2